*Journal of Zoological Systematics and Evolutionary Research*

WILEY

RESEARCH ARTICLE OPEN ACCESS

# New Species and Phylogeny of *Alentiana* Hartman, 1942 (Annelida, Polynoidae) Reveal Polyphyly of Lepidastheniinae and Key Morphological Character Evolution

Xuwen Wu[1,2] | Qi Kou[1,2] | Yu Li[1,2] | Kuidong Xu[1,2,3]

[1]Laboratory of Marine Organism Taxonomy and Phylogeny, Shandong Province Key Laboratory of Marine Biodiversity and Bio-resource Sustainable Utilization, Institute of Oceanology, Chinese Academy of Sciences, Qingdao 266071, China | [2]University of Chinese Academy of Sciences, Beijing 100049, China | [3]Laboratory for Marine Biology and Biotechnology, Qingdao Marine Science and Technology Center, Qingdao 266071, China

**Correspondence:** Kuidong Xu (kxu@qdio.ac.cn)

**Received:** 4 February 2026 | **Revised:** 2 March 2026 | **Accepted:** 5 March 2026

**Academic Editor:** Savel Daniels

## ABSTRACT

*Alentiana*, a genus within the subfamily Lepidastheniinae of Polynoidae, is an obligately commensal deep-sea group exclusively associated with sea anemones. Currently, only two valid species are recognized, with the genus's species diversity and phylogenetic relationships remaining poorly understood. In this study, we systematically investigated polynoid specimens collected from four seamounts in the tropical western Pacific. Integrating morphological observations (including SEM observations of chaetal ultrastructure) and genome skimming data, we describe two new species: *Alentiana barnichae* sp. nov. and *A. fiegei* sp. nov., clarifying their morphological diagnostic characters and body size-related intraspecific variations. Phylogenetic analyses based on 13 mitochondrial protein-coding genes and four ribosomal genes revealed that *Alentiana* forms a well-supported monophyletic clade, which is sister to the deep-sea subfamily Macellicephalinae but not closely related to other genera traditionally assigned to Lepidastheniinae. Lepidastheniinae was clearly recovered as polyphyletic, and notably, it shares terminally inserted lateral antennae with Lepidonotinae without exhibiting a close phylogenetic relationship, thus challenging the reliability of traditional taxonomic characters. Ancestral state reconstruction indicated that terminally or subterminally inserted lateral antennae represent a plesiomorphy of Polynoidae, while deeply incised neuropodia are a product of convergent evolution presumably driven by ecological pressures and cannot serve as an exclusive diagnostic character for Lepidastheniinae. This study enriches the species diversity and geographical distribution records of *Alentiana*, clarifies its phylogenetic position, and provides insights for revising the taxonomic system of Polynoidae and understanding the evolution of key morphological traits.

## 1 | Introduction

The family Polynoidae Kinberg, 1856 [1] is a key group for investigating commensal ecological relationships among polychaete annelids [2–4]. According to Martin and Britayev [2], this family comprises 219 commensal species belonging to 79 genera, accounting for over 45% of all known symbiotic polychaetes. Among its subfamilies, Lepidastheniinae Pettibone, 1989 [5] includes the genus *Alentiana* Hartman, 1942 [6], which comprises obligate deep-sea polynoids exclusively commensal with sea anemones. This symbiotic association is rarely documented within Polynoidae.

Xuwen Wu and Qi Kou contributed equally to this work.

To date, only two valid species of *Alentiana* are recognized: *A. aurantiaca* (Verrill, 1885) [7] was recorded from coastal waters off the northeastern USA at depths of 347–1170 m [6, 8], while *A. palinpoda* Wang et al., 2021 [9] was described from a seamount in the northwestern Pacific at a depth of 1156 m [9]. Although Amoureux [10] reported *A. aurantiaca* from European waters, Barnich (WoRMS taxonomic editor for this genus; in Read and Fauchald [11]) stated that this record is likely a misidentification and requires verification via examination of voucher specimens, based on her taxonomic examinations of Mediterranean polynoid fauna (e.g., [12]). These sparse and scattered records directly reflect our limited understanding of its species diversity, highlighting the need for targeted sampling in understudied areas (e.g., tropical western Pacific seamounts).

Among the subfamilies of Polynoidae, Lepidastheniinae and Lepidonotinae have long been regarded as closely related due to their morphological similarities. Specifically, both possess a pair of terminally inserted lateral antennae [12–16]. The key diagnostic differences between the two subfamilies lie in the morphology of neuropodia and dorsal tubercles: Lepidastheniinae exhibit neuropodia deeply incised dorsally and ventrally (with prechaetal and postchaetal lobes of similar size and shape) and indistinct dorsal tubercles, while Lepidonotinae lack deeply incised neuropodia and have distinct dorsal tubercles. Based on these clear differences, Pettibone [5] segregated six genera from Lepidonotinae, formally establishing the subfamily Lepidastheniinae. The subfamily currently comprises 12 genera [11]. To date, no studies have explicitly focused on the relationship between Lepidastheniinae and Lepidonotinae, but recent molecular phylogenetic studies on the polynoid groups (e.g., [17–20]) have revealed that some Lepidastheniinae species are nested within Lepidonotinae clades, thus challenging the monophyly of Lepidastheniinae and blurring subfamily boundaries. Accordingly, the phylogenetic relationship between Lepidastheniinae and Lepidonotinae remains poorly resolved to date because molecular data for Lepidastheniinae remain extremely limited. This necessitates verifying the monophyly of Lepidastheniinae, resolving its phylogenetic position within Polynoidae, and re-evaluating the reliability of traditional key diagnostic traits for distinguishing these subfamilies (i.e., terminally inserted lateral antennae and deeply incised neuropodia).

A detailed examination of polychaete specimens recently collected from four tropical western Pacific seamounts revealed two new species of *Alentiana*: *A. barnichae* sp. nov. and *A. fiegei* sp. nov. The mitochondrial genome and nuclear ribosome RNA sequences of the new species were obtained through the genome-skimming sequencing approach (12S, 16S, 18S, and 28S rRNA). Combining these newly generated data with existing public sequences enabled phylogenetic analyses of Polynoidae. The aim of this study is threefold: (1) to describe the morphology of the new species in detail, including intraspecific variations associated with body size; (2) to verify the monophyly of *Alentiana* and its associated subfamily, and to clarify their phylogenetic positions within Polynoidae; and (3) to explore the evolutionary patterns of key morphological traits (e.g., parapodial structure and terminally inserted lateral antennae).

## 2 | Materials and Methods

### 2.1 | Acquisition of Materials and Morphological Observation Methods

#### 2.1.1 | Sample Collection

All *Alentiana* specimens were collected from four deep-sea seamounts in the tropical western Pacific (tentatively named seamounts M4, M5, M8, and Seamount Kocebu) via the remotely operated vehicle (ROV) *FaXian* aboard the research vessel (R/V)*KeXue*, during four dives between August 2017 and June 2019. Among these four seamounts, M4, M5, and M8 are adjacent to each other and all located in the Caroline Seamount Chain, while Seamount Kocebu is situated northeast of the three seamounts, ~1700 km away from them (Figure S1). Most specimens were obtained by collecting host sea anemones with the ROV manipulator. The ROV simultaneously captured in situ photographs of the symbiotic association between *Alentiana* specimens and their host sea anemones during sampling. *Alentiana* individuals were subsequently isolated from contracted host anemones in the laboratory after collection.

*Alentiana* specimens may detach from their hosts, or host sea anemones may be lost, during ROV sampling, operation, and recovery. Consequently, direct specimen–host matching cannot be conducted during subsequent sorting. However, indirect matching of most specimens to their respective hosts was accomplished using the in-situ photographs and field collection records. Detailed information for all specimens, including specimen numbers, species identities, associated host anemones, dive records, collection coordinates (longitude and latitude), sampling depth, collection date, and notes, is summarized in Table 1.

#### 2.1.2 | Specimen Preservation and Deposition

Immediately after collection, all specimens were fixed and preserved in 80% (v/v) ethanol solution to maintain morphological integrity. All specimens were subsequently deposited in the Marine Biological Museum of the Chinese Academy of Sciences (MBMCAS), affiliated with the Institute of Oceanology, Chinese Academy of Sciences (IOCAS).

It should be noted that specimen MBM287246 dried out due to alcohol leakage during preservation. This desiccation made it impossible to observe its morphology, and all subsequent attempts at genetic sequencing for this specimen also failed. Consequently, the present study only provides pre-desiccation dorsal and ventral photographs of the specimen, in situ photographs of its symbiotic association with sea anemones, and complete collection information for this specimen. This specimen is included in the present study because it provides detailed collection information for *Alentiana*, thus supplementing its known distribution and ecological records.

#### 2.1.3 | Morphological Observation and Photography

A Sony Alpha 7R IV mirrorless camera fitted with a Laowa FF 100 mm f/2.8 2× macro lens was used to capture the overall morphology of all specimens, clearly documenting body size, body color, and general morphological characteristics. Key taxonomic characters (head, elytra, pygidium, and parapodia) were stained with methyl green solution where necessary to enhance the

**TABLE 1** | Information table of *Alentiana* (polynoidae) specimens involved in the study.

| Specimen no. | Species name | Host anemone | Dive no. | Seamount | Longitude | Latitude | Depth (m) | Collection Date | Notes |
|---|---|---|---|---|---|---|---|---|---|
| MBM286814 | *Alentiana barnichae* sp. nov. | Unconfirmed | Dive 142 | M4 | 140°10′E | 10°31′N | ~1100 m | August 25, 2017 | Holotype |
| MBM287245 | *Alentiana barnichae* sp. nov. | *Bolocera* sp. | Dive 142 | M4 | 140°10′46″E | 10°31′14″N | 1156 m | August 25, 2017 | Paratype |
| MBM286815 | *Alentiana barnichae* sp. nov. | *Sicyonis* sp1. | Dive 221 | M5 | 140°08′52″E | 10°02′54″N | 2291 m | June 9, 2019 | Paratype |
| MBM287243 | *Alentiana fiegei* sp. nov. | *Sicyonis* sp2. | Dive 142 | M4 | 140°10′54″E | 10°31′18″N | 1219.1 m | August 25, 2017 | Holotype |
| MBM287244 | *Alentiana fiegei* sp. nov. | *Sicyonis* sp2. | Dive 224 | M8 | 140°05′01″E | 10°36′55″N | 871 m | June 12, 2019 | Paratype |
| MBM287246 | *Alentiana* sp. | *Bolocera* sp. | Dive 174 | Kocebu | 153°13′46″E | 17°29′20″N | 1301.9 m | April 8, 2018 | Dried out |

contrast of morphological details, then observed under a Zeiss Discovery V12 stereomicroscope. Microscopic images of these characters were acquired using the same Sony Alpha 7R IV camera mounted on the stereomicroscope. Parapodial chaetae from each specimen were selected for ultrastructural observation, following standard protocols: (1) Isolated parapodia were rinsed with absolute ethanol to remove residual fixative and debris; (2) Samples were dehydrated in a graded ethanol series (30%, 50%, 70%, 80%, 90%, 95%, 100% v/v) for 15 min per gradient; (3) Dehydrated samples were critical-point dried with liquid $CO_2$ and sputter-coated with a thin 10 nm gold layer. Ultrastructural features of chaetae (e.g., surface spines, terminal structures) were subsequently observed and imaged using a Hitachi S-3400N scanning electron microscope (Hitachi High-Technologies Corporation, Tokyo, Japan), yielding high-resolution morphological evidence for species delimitation.

To resolve fine morphological details across different focal planes (e.g., posterior segments, parapodial lobes, pharyngeal distal papillae) in the acquired micrographs, multi-focal-plane images were merged using Helicon Focus 7 software. For species exhibiting intraspecific morphological variation associated with body size, morphological traits (e.g., color bands, parapodial development, elytral, and segment counts) of individuals with different body lengths were compared to delineate the intraspecific morphological variation range of the species.

## 2.2 | Molecular Analyses

### 2.2.1 | Genetic Data Generation

Genetic data were newly obtained from five individuals of the two new species for phylogenetic inference. Genomic DNA was extracted from a small piece of muscle tissue (~10 mg) with QIAamp DNA Micro Kit (Qiagen, Hilden, Germany) following the manufacturer's instructions. The DNA was eluted in 100 μL of sterile distilled $H_2O$ (RNase free), and quantified by 1.5% agarose gel electrophoresis and using the NanoPhotometer N60 (Implen, Munich, Germany).

The extracted genomic DNA (0.1–1 μg) was sent to Berry Genomics Co., Ltd (Beijing, China) for whole genome sequencing (WGS). Paired-end libraries with an insert size of 350 bp were sequenced ($2 \times 150$ bp) on the DNBSEQ-T7 platform (MGI, Shenzhen, China). Approximately 6 Gb of raw data were produced for each library.

### 2.2.2 | De Novo Assembly and Sequences Extraction

Prior to assembly, raw reads were filtered to remove adaptors and low-quality reads using Trimmomatic 0.39 [21]. Genome contigs were assembled with multiple *k*-mer strategies ($k = 21, 29, 39, 59, 79, 99, 119, 141$) using MegaHit 1.2.9 [22] due to its ultra-fast speed and low computing resource cost. All the assemblies were executed on a workstation with 20 cores and 128G memory. Subsequently, contigs including mitochondrial genome and nuclear ribosome were identified by similarity search using BLAST + 2.12.0 [23] with *e*-value $\leq 1e{-}06$ against corresponding reference sequences of other polynoids (Table 2). Then, sequences of 13 mitochondrial protein coding genes (PCGs), 12S, 16S, 18S, and 28S were extracted, respectively, by mapping

**TABLE 2** | Species used for constructing the genome-skimming tree with NCBI accession numbers.

| Family | Subfamily | Species | Voucher ID | Mitogenome | 18S rRNA | 28S rRNA |
|---|---|---|---|---|---|---|
| Polynoidae | Admetellinae | *Admetella levensteini* | MBM-286807 | PQ221480 | PQ211133 | PQ211133 |
| | | *Admetella multiseta* | MBM-286065 | PQ221478 | PQ211131 | PQ211131 |
| | | *Admetella nanhaiensis* | MBM-286808 | PQ221483 | PQ211136 | PQ211136 |
| | | *Admetella undulata* | MBM-286809 | PQ221482 | PQ211135 | PQ211135 |
| | Arctonoinae | *Arctonoe vittata* | SAMN40631062 | SRR28477832 | SRR28477832 | SRR28477832 |
| | | *Gastrolepidia clavigera* | SMNH-118964 | OZ318083 | JN852825 | JN852855 |
| | Eulagiscinae | *Eulagisca gigantea* | SIO-BIC-A6302 | SRR25320644 | SRR25320644 | SRR25320644 |
| | Lepidastheniinae | *Alentiana palinpoda* | B6317500003 | [a] | MW397195 | MW412252 |
| | | *Alentiana barnichae* sp. nov. | MBM-286815 | **SRR37048088** | **SRR37048088** | **SRR37048088** |
| | | *Alentiana fiegei* sp. nov. | MBM-287244 | **SRR37048087** | **SRR37048087** | **SRR37048087** |
| | | *Hyperhalosydna striata* | SMNH-118971 | MW620990 | JN852831 | JN852862 |
| | | *Lepidasthenia elegans* | SMNH-118973 | [b] | JN852832 | JN852863 |
| | Lepidonotinae | *Alentia gelatinosa* | SAMEA9926053 | CATLOO010000000 | CATLOO000000000 | CATLOO000000000 |
| | | *Halosydna brevisetosa* | SAMEA112639153 | ERR13493957 | ERR13493957 | ERR13493957 |
| | | *Halosydna* sp. | YZ-2018 | KY753830 | KY753845 | KY753845 |
| | | *Lepidonotus clava* | SAMN21849802 | SRR16188824 | SRR16188824 | SRR16188824 |
| | | *Lepidonotus* sp. | YZ-2018 | KY753831 | KY753851 | KY753851 |
| | Macellicephalinae | *Bathykurila* sp. | SIO-BIC-A10920 | SRR25320650 | SRR25320650 | SRR25320650 |
| | | *Branchiplicatus cupreus* | SIO-BIC-A6160 | SRR25320645 | SRR25320645 | SRR25320645 |
| | | *Branchinotogluma hessleri* | SIO-BIC-A12940 | SRR25320649 | SRR25320649 | SRR25320649 |
| | | *Branchipolynoe japonicus* | HPD1858-BC4-11 | KY753824 | KY753841 | KY753841 |
| | | *Branchipolynoe longqiensis* | JC67-f-033/1b | KY753826 | KY753847 | KY753847 |
| | | *Branchipolynoe pettiboneae* | N/A | KY753825 | KY753840 | KY753840 |
| | | *Branchipolynoe segonzaci* | SAMN21601035 | SRR16188828 | SRR16188828 | SRR16188828 |
| | | *Cladopolynoe tunnicliffeae* | SIO-BIC-A7717 | SRR25320646 | SRR25320646 | SRR25320646 |
| | | *Gesiella jameensis* | N/A | MW794260 | MW794263 | MW794263 |
| | | *Lepidonotopodium fimbriatum* | SIO-BIC-A6153 | SRR25320642 | SRR25320642 | SRR25320642 |
| | | *Levensteiniella kincaidi* | SIO-BIC-A6310 | SRR25320637 | SRR25320637 | SRR25320637 |
| | | *Macellicephala* sp. 1 | SIO-BIC-A11031 | SRR25320635 | SRR25320635 | SRR25320635 |
| | | *Macellicephala* sp. 2 | SIO-BIC-A3432 | SRR25320634 | SRR25320634 | SRR25320634 |
| | | *Macellicephala* sp. 3 | SIO-BIC-A10055 | SRR25320633 | SRR25320633 | SRR25320633 |
| | | *Macellicephala* sp. 4 | SIO-BIC-A10099 | SRR25320632 | SRR25320632 | SRR25320632 |

(Continues)

**TABLE 2** | (Continued)

| Family | Subfamily | Species | Voucher ID | Mitogenome | 18S rRNA | 28S rRNA |
|---|---|---|---|---|---|---|
| | | *Macellicephaloides lingshuiensis* | MBM-286812 | PX118544 | PX132557 | PX132557 |
| | | *Mamiwata piscesae* | SIO-BIC-A7978 | SRR25320641 | SRR25320641 | SRR25320641 |
| | | *Peinaleopolynoe orphanae* | SIO-BIC-A6163 | SRR25320629 | SRR25320629 | SRR25320629 |
| | | *Pelagomacellicephala iliffei* | N/A | MW794261 | MW794264 | MW794264 |
| | | *Photinopolynoe lunae* | SIO-BIC-A13248 | SRR25320648 | SRR25320648 | SRR25320648 |
| | | *Stratigos theoi* | MCZ-IZ-68096 | SRR25320624 | SRR25320624 | SRR25320624 |
| | | *Themis intermedia* | SIO-BIC-A13187 | SRR25320639 | SRR25320639 | SRR25320639 |
| | | *Thermopolynoe branchiata* | SIO-BIC-A10925 | SRR25320626 | SRR25320626 | SRR25320626 |
| | Polynoinae | *Acholoe squamosa* | SAMEA13854387 | CASGGO000000000 | CASGGO000000000 | CASGGO000000000 |
| | | *Eunoe nodosa* | SAMN17766237 | SRR14996616 | SRR14996616 | SRR14996616 |
| | | *Harmothoe impar* | SAMEA8419683 | CANHQH000000000 | CANHQH000000000 | CANHQH000000000 |
| | | *Melaenis* sp. | YZ-2018 | KY753829 | KY753849 | KY753849 |
| | | *Pettitbonesia furcosetosa* | SAMN21849801 | SRR16188832 | SRR16188832 | SRR16188832 |
| | | *Polyeunoa laevis* | NSJC66-477-S001 | MN057924 | KU738176 | KU738193 |
| Acoetidae | | *Panthalis oerstedi* | A5344 | KY753832 | KY753846 | KY753846 |
| Aphroditidae | | *Laetmonice producta* | A2989 | KY753833 | KY753853 | KY753853 |
| Eulepethidae | | *Eulepethus nanhaiensis* | AMW-49067 | KY753834 | KY753850 | KY753850 |
| Iphionidae | | *Iphione* sp. | YZ-2018 | KY753835 | KY753852 | KY753852 |
| Sigalionidae | Pholoinae | *Pholoe pallida* | A6209 | KY753838 | KY753843 | KY753843 |
| | Pisioninae | *Pisione galapagoensis* | SAMN14489989 | SRR12246727 | SRR12246727 | SRR12246727 |
| | | *Pisionidens* sp. | SAMN14489988 | SRR12246780 | SRR12246780 | SRR12246780 |
| | Sigalioninae | *Euthalenessa festiva* | A2819 | KY753837 | KY753839 | KY753839 |
| | | *Sthenelais limicola* | SAMEA8724794 | CALNXG000000000 | CALNXG000000000 | CALNXG000000000 |

*Note:* New sequencing data are in bold.
[a]Only 16S rRNA (MW397208) and COI (MW374288) sequences available and included;
[b]Only 16S rRNA (JN852901) and COI (JN852933) sequences available and included.

to corresponding reference sequences using Unipro UGENE 42.0 [24].

#### 2.2.3 | Phylogenetic Analyses

Two mitochondrial genes, 16S and COI, were used for interspecific genetic distances comparisons among the three species of *Alentiana*. The Kimura's 2-parameter genetic distances were calculated using MEGA 6.06 [25].

To explore the internal relationships and the morphological character evolution patterns of polynoids, a matrix consisting of 13 mitochondrial PCGs, 12S, 16S, 18S, and 28S gene sequences was used to infer the phylogeny of Polynoidae. The ingroup comprised the two new species and additional 44 species from seven subfamilies, while nine species from the other five families of Aphroditiformia Levinsen, 1883 [26] were selected as outgroup (Table 2). Except for *Alentiana palinpoda* and *Lepidasthenia elegans* (Grube, 1840)[27], for which only 16S, COI, 18S and 28S genes were available, the 13 mitochondrial PCGs, 12S, 16S, 18S, and 28S gene sequences of other 53 species were obtained via either downloaded from GenBank or extracted from assemblies based on raw WGS data deposited at NCBI Sequence Read Archive (SRA) database. Genome contigs assembly and target genes extraction procedures were the same as described above.

Extracted homologous gene sequences were aligned using Clustal Omega 1.2.4 [28] implemented in UGENE 42.0 with default parameters, followed by manual trimming to ensure uniform length across all taxa. The highly divergent and poorly aligned segments of each ribosomal gene alignment were removed using GBlocks 0.91b [29] before phylogenetic tree reconstructions (GBlocks parameters: minimum length of a block = 5; allowed gap positions = with half). Then the trimmed alignments were concatenated into a matrix using Sequence Matrix 1.8 [30]. Phylogenetic trees were constructed using maximum likelihood (ML) and Bayesian inference (BI) methods. The matrices were partitioned by gene, as well as three codon positions for each PCG. The best-fit substitution models and partitioning schemes for ML and BI analyses were selected separately by ModelFinder [31] implemented in IQ-TREE 2.2.0.3 [32], which were applied to follow-up corresponding analysis. The best-fit substitution models and partitioning schemes for ML and BI analyses (Table S1). The ML trees were inferred using IQ-TREE 2, and branch supports were assessed by performing SH-aLRT branch test [33] as well as ultrafast bootstrap (UFBoot) [34] with 10,000 replicates. The BI trees were reconstructed using MrBayes 3.2.6 [35] with two independent runs of four Markov Chains for 10,000,000 generations and sampling every 1000 generations. After the first 25% trees were discarded as burn-in, the remaining trees were used to generate the 50% majority rule consensus tree and estimate the posterior probabilities (PP). The effective sample size (ESS) values for all sampled parameters and the average standard deviation of split frequencies (ASDSF) were assessed using Tracer 1.7.1 [36] to ensure convergence (ESS > 200, ASDSF < 0.01). The phylogenetic trees were visualized using FigTree 1.4.3 [37] and annotated with Adobe Photoshop CS4.

#### 2.2.4 | Ancestral State Reconstruction

Four characters concerning lateral antennae and parapodia of the studied polynoid species were summarized for phylogenetic analysis (Table S2). Ancestral states were reconstructed via stochastic character mapping using the empirical Bayes method. PPs of the ancestral states were generated from 100 stochastic character maps for each trait using the *make.simmap* function in the R package "phytools" [38]. Reconstructions were based on the topology inferred from BI analyses of the fully partitioned Sanger sequencing dataset. Finally, stochastic character maps for each trait were plotted onto the inferred phylogeny, with PPs displayed at each node (pie charts).

Specifically, morphological characters and their corresponding coded states were defined as follows: Lateral antennae: State 0 = absent; State 1 = present. Lateral antennae terminally or subterminally inserted: State 0 = absent; State 1 = present. Lateral antennae ventrally or terminoventrally inserted: State 0 = absent; State 1 = present. Deeply incised neuropodia: State 0 = absent; State 1 = present.

## 3 | Results

### 3.1 | Genetic Distance and Phylogenetic Analyses

Kimura's two-parameter (K2P) genetic distances were estimated for the 16S rRNA (528 bp; Table S3, below diagonal) and COI (1540 bp; Table S3, above diagonal) gene sequences of three *Alentiana* species.

For the 16S rRNA gene, intraspecific genetic divergences within *Alentiana* ranged from 0.00% to 0.57% (0.00%–0.57% in *A. barnichae* sp. nov., 0.00% in *A. fiegei* sp. nov.), while interspecific divergences among the three *Alentiana* species ranged from 0.76% (*A. barnichae* sp. nov. vs. *A. fiegei* sp. nov., *A. fiegei* sp. nov. vs. *A. palinpoda*) to 1.34% (*A. barnichae* sp. nov. vs. *A. palinpoda*). For the COI gene, intraspecific divergences ranged from 0.00% to 1.05% (0.00%–1.05% in *A. barnichae* sp. nov., 0.26% in *A. fiegei* sp. nov.), and interspecific divergences ranged from 3.48% (*A. barnichae* sp. nov. vs. *A. palinpoda*) to 5.72% (*A. fiegei* sp. nov. vs. *A. palinpoda*).

These genetic divergence patterns were consistent with the observed morphological differentiation among the three species, supporting their delimitation as distinct taxa.

The final 17-gene matrix derived from the genome-skimming data consists of 17,475 bp (~87.18% of the original 20,045 bp alignment) after the poorly aligned positions and hyper-variable regions were removed using Gblocks (original alignments of 12S/16S/18S/28S = 857/1168/2157/4721 bp, trimmed alignments of 12S/16S/18S/28S = 608/811/1762/3152 bp). The optimum partitioning schemes and the best-fit models for each partitioned subset selected by ModelFinder are listed in Table S1. After 10 million iterations, the ASDSF in BI analysis reached below 0.002, and the ESS values for all sampled parameters were above 1000 for each run.

Except for a few internal nodes, the topologies generated from ML and BI analyses are highly congruent and well-supported (Figure 1; Figures S2, S3). The phylogenetic tree revealed that *Alentiana* constitutes a well-supported monophyletic clade, a finding consistent with the genus's shared morphological characteristics and relatively low interspecific genetic distances. However, rather than clustering with other genera formally assigned to the subfamily Lepidastheniinae, *Alentiana* formed a sister group to the deep-sea subfamily Macellicephalinae Hartmann-Schröder, 1971 [39], and these two clades together constituted a distinct lineage.


**FIGURE 1** | Bayesian inference tree of Polynoidae inferred from the concatenated 17-gene matrix partitioned by gene and codon. Nodal supports are denoted on the corresponding branches as specified in the legend in the top-left corner.

The subfamily Lepidastheniinae was recovered as polyphyletic, with its representative species distributed across disparate clades in the phylogeny. In addition to *Alentiana*'s affiliation with Macellicephalinae, *Lepidasthenia elegans* was resolved as sister to the clade comprising Polynoinae Kinberg, 1856 [1] and Arctonoinae Hanley, 1989 [40], while *Hyperhalosydna striata* (Kinberg, 1856) [1] (also formally assigned to Lepidastheniinae) was nested within a well-supported major clade of Lepidonotinae Willey, 1902 [41].

The subfamily Lepidonotinae was also recovered as polyphyletic. *Alentia gelatinosa* (M. Sars,1835)[42] is sister to *Eulagisca gigantea* Monroe, 1939 [43] (a representative of the subfamily Eulagiscinae Pettibone, 1997 [44]), instead of falling into the major clade of Lepidonotinae.

In contrast, the subfamilies Macellicephalinae, Polynoinae, Arctonoinae, and Admetellinae Uschakov, 1977 [45] were each recovered as well-supported monophyletic clades.

## 3.2 | Ancestral State Reconstruction (Figure 2)

Most Polynoidae species possess distinct lateral antennae (albeit with varying insertion positions), while the absence of lateral antennae is restricted to the subfamily Macellicephalinae. Ancestral state reconstruction demonstrated that the presence of lateral antennae is a plesiomorphy of Polynoidae, whereas the absence of lateral antennae constitutes a synapomorphy of Macellicephalinae.

Our analyses demonstrated that terminally or subterminally inserted lateral antennae occur not only in the subfamilies Lepidastheniinae and Lepidonotinae but also in smaller subfamilies such as Admetellinae and Eulagiscinae. This insertion pattern represents a putative plesiomorphy of Polynoidae, with all other lateral antenna insertion phenotypes (including ventrally/terminoventrally inserted lateral antennae and the absence of lateral antennae) representing derived states from this ancestral condition.

Ventrally and terminoventrally inserted lateral antennae are represented in the subfamilies Polynoinae and Arctonoinae, respectively. The ventral or terminoventral insertion character represents a clear synapomorphy of the clade comprising the subfamilies Polynoinae and Arctonoinae.

Within Polynoidae, deeply incised neuropodia are absent in most species, being restricted to four distinct clades. Three of these clades belong to Lepidastheniinae, while the fourth corresponds

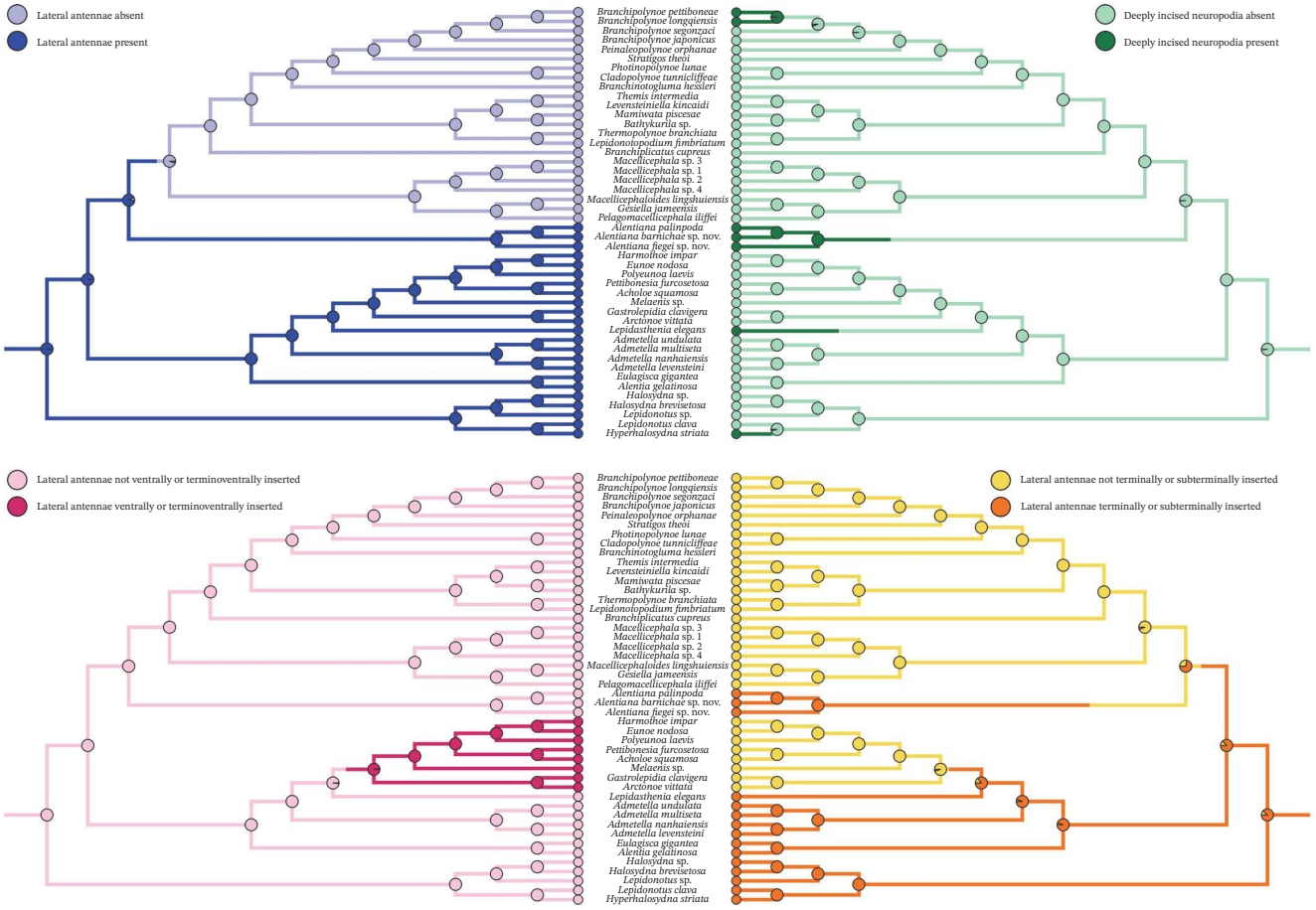


**FIGURE 2** | Ancestral state reconstructions of four characters of polynoids concerning lateral antennae and parapodia based on the BI tree inferred from the concatenated 17-gene matrix. Trees are shown in duplicate tips-to-tips, and the posterior probabilities of different ancestral states are indicated by the pie chart on the corresponding nodes.

to the genus *Branchipolynoe* Pettibone, 1984 [46] (Macellicephalinae), a polynoid taxon symbiotic with deep-sea mussels in chemosynthetic habitats.

Our analyses further demonstrated that the absence of deeply incised neuropodia represents a plesiomorphy of Polynoidae, and that deeply incised neuropodia in these four clades represent a product of convergent evolution (homoplasy), and thus cannot function as a diagnostic synapomorphy for delimiting Lepidastheniinae.

## 3.3 | Systematics

Class Polychaeta Grube, 1850 [47].

Order Phyllodocida Dales, 1962 [48].

Family Polynoidae Kinberg, 1856 [1].

### 3.3.1 | *Genus Alentiana Hartman, 1942*

**Type species.** *Alentiana aurantiaca* (Verrill, 1885) [7].

**Diagnosis**. Body oval, flattened, length up to 50 mm, with variable number of segments (30–39) depending on body size, last few segments very small.

Prostomium with four distinct eyes, two long palps and three antennae (one median and two lateral); median antenna with large ceratophore; lateral antennae slender with smaller ceratophore, inserted on anterolateral extensions of prostomium. Muscular pharynx with two pairs of jaws, nine pairs of distal papillae and two pairs of lateral papillae. Tentacular segment (first segment) achaetous, with two pairs of tentacular cirri inserted laterally to prostomium.

Elytra smooth, covering dorsum or leaving median dorsum exposed; 14–20 pairs, arranged on segments 2, 4, 5, 7, alternately to 23, then on every third segment up to 35, and then on every segment up to 39. Dorsal tubercles slightly nodular conical, or indistinct. Parapodia sub-biramous. Dorsal cirri with cylindrical cirrophores and tapering styles. Notopodia reduced as a conical lobe, without notochaetae. Neuropodia well developed, either ovate, short-subtriangular, or long-digitiform; deeply incised dorsally and ventrally, with prechaetal lobe and postchaetal lobe of similar size and shape. Neuropodia with two kinds of neurochaetae: a fascicle of slender, slightly serrated supraacicular chaetae and one to two thick, spinous subacicular hooks. Ventral cirri tapering, inserted basally on neuropodia, larger and thicker on segment 2, becoming smaller on subsequent segments. Nephridial papillae small, ovate, or indistinct. Pygidium enclosed by 2 or 3 smaller posterior segments, with a pair of anal cirri.

**Remarks.** Morphologically, *Alentiana* is readily distinguishable from other genera within Lepidastheniinae by the following key diagnostic features: the notopodia are significantly reduced and

lack notochaetae, while the neuropodia are well developed and bear a fascicle of slender, slightly serrated supraacicular chaetae and one to two thick, spinous subacicular hooks.

The terminal segments and elytra of *Alentiana* species are extremely fragile. Elytra are easily detached, and some individuals display posterior body fragmentation and regeneration. These factors hinder accurate counting of segments and elytra, leading to inconsistencies in historical descriptions. When describing *A. aurantiaca*, Hartman [6] reported approximate counts of segments (c. 39) and elytra (18 pairs or more), and noted that its elytra extend to segments 34, 36, and 37. In contrast, Pettibone [8] recorded 17–20 pairs of elytra for this species, with their elytra extent inferred to reach segments 39. These discrepancies are likely due to incomplete development of terminal segments and their elytra; such delicate structures are easily overlooked during routine microscopic examinations.

Nephridial papillae constitute a diagnostic feature for species delimitation within *Alentiana* and are herein incorporated into the generic diagnosis. Early taxonomists who established *Alentiana* and examined numerous *A. aurantiaca* specimens provided no account of nephridial papillae [6, 8], implying their absence or indistinctness in this species. By contrast, Wang et al. [9] clearly documented that nephridial papillae first occur on segment 4 in *A. palinpoda*, the second species described in the genus. The present study observes that nephridial papillae begin on segment 10 in *A. barnichae*. These distinctions indicate that nephridial papillae serve as a diagnostic character for species recognition within *Alentiana*.

Furthermore, dorsal tubercle morphology represents an additional component of the revised diagnosis of *Alentiana*. Traditionally, the presence and development of dorsal tubercles have been used to distinguish the subfamilies Lepidastheniinae and Lepidonotinae: Lepidastheniinae lacks conspicuous dorsal tubercles or bearing only indistinct ones, while Lepidonotinae possesses dorsal tubercles of variable sizes. As *Alentiana* has long been placed in Lepidastheniinae, previous generic diagnoses described the genus as lacking conspicuous dorsal tubercles or having only indistinct ones. However, examination of our specimens revealed interspecific variation in dorsal tubercle morphology within *Alentiana*: some species (e.g., *A. barnichae* and *A. fiegei*) have small, well-defined nodular or conical dorsal tubercles, whereas others (e.g., *A. palinpoda*) have indistinct ones. Based on these observations, we have revised the description of dorsal tubercles in the generic diagnosis, documented their interspecific variation, and propose that dorsal tubercles should not serve as a taxonomic criterion to distinguish these two subfamilies.

### 3.3.2 | *Alentiana barnichae* sp. nov. (Figures 3–7)

**Material examined.** Holotype: MBM286814, Dive 142, M4 seamount (140°10′E, 10°31′N), ~1100 m, August 25, 2017. Paratype: MBM287245, Dive 142, M4 seamount (140°10′46″E, 10°31′14″N),

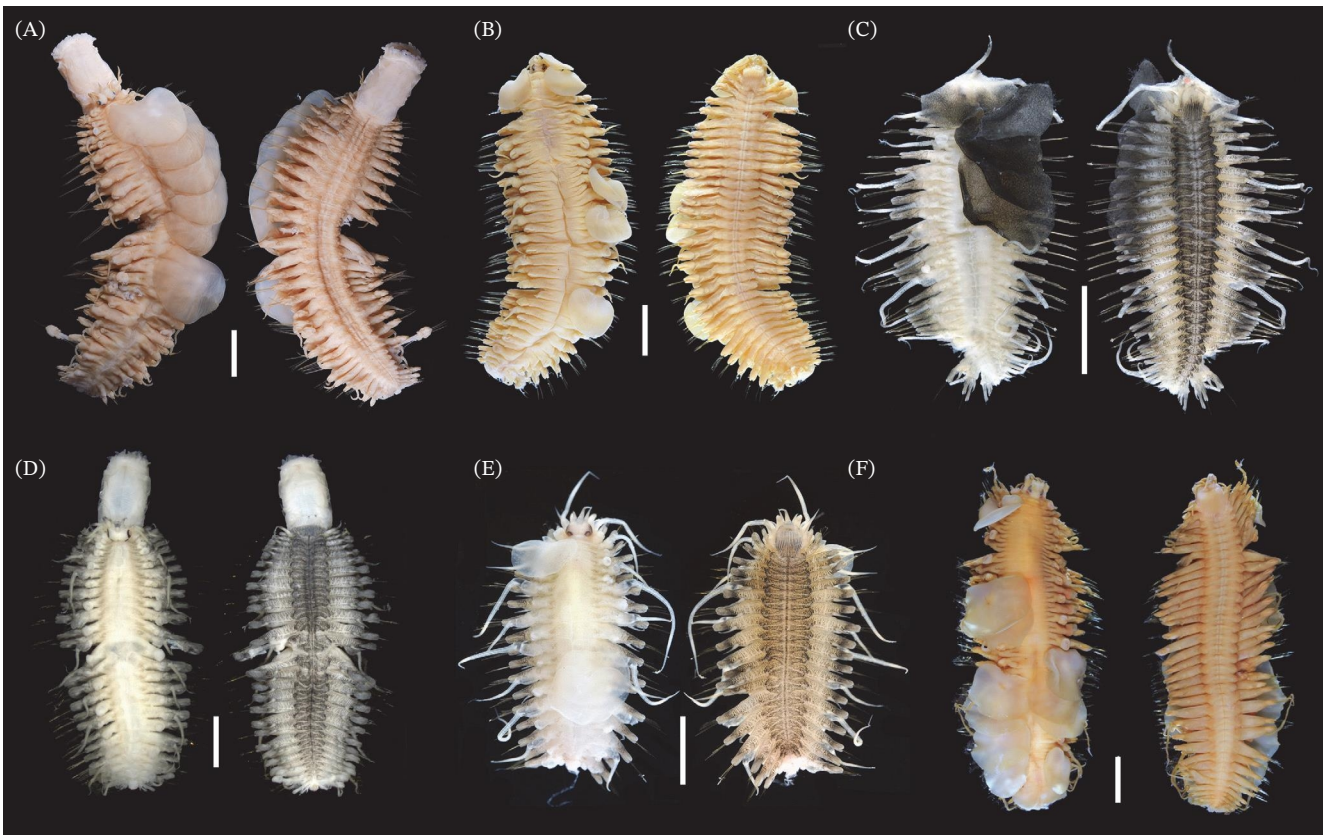


**FIGURE 3** | Preserved specimens of *Alentiana* in dorsal and ventral view. (A) *Alentiana barnichae* sp. nov., holotype (MBM286814); (B) *A. barnichae* sp. nov., paratype (MBM287245); (C) *A. barnichae* sp. nov., paratype (MBM286815); (D) *A. fiegei* sp. nov., holotype (MBM287243); (E) *A. fiegei* sp. nov., paratype (MBM287244); (F) *A.* sp. (MBM287246, Dried out by alcohol evaporation). Scale bars: 5 mm (A, B, F) and 2 mm (C–E).

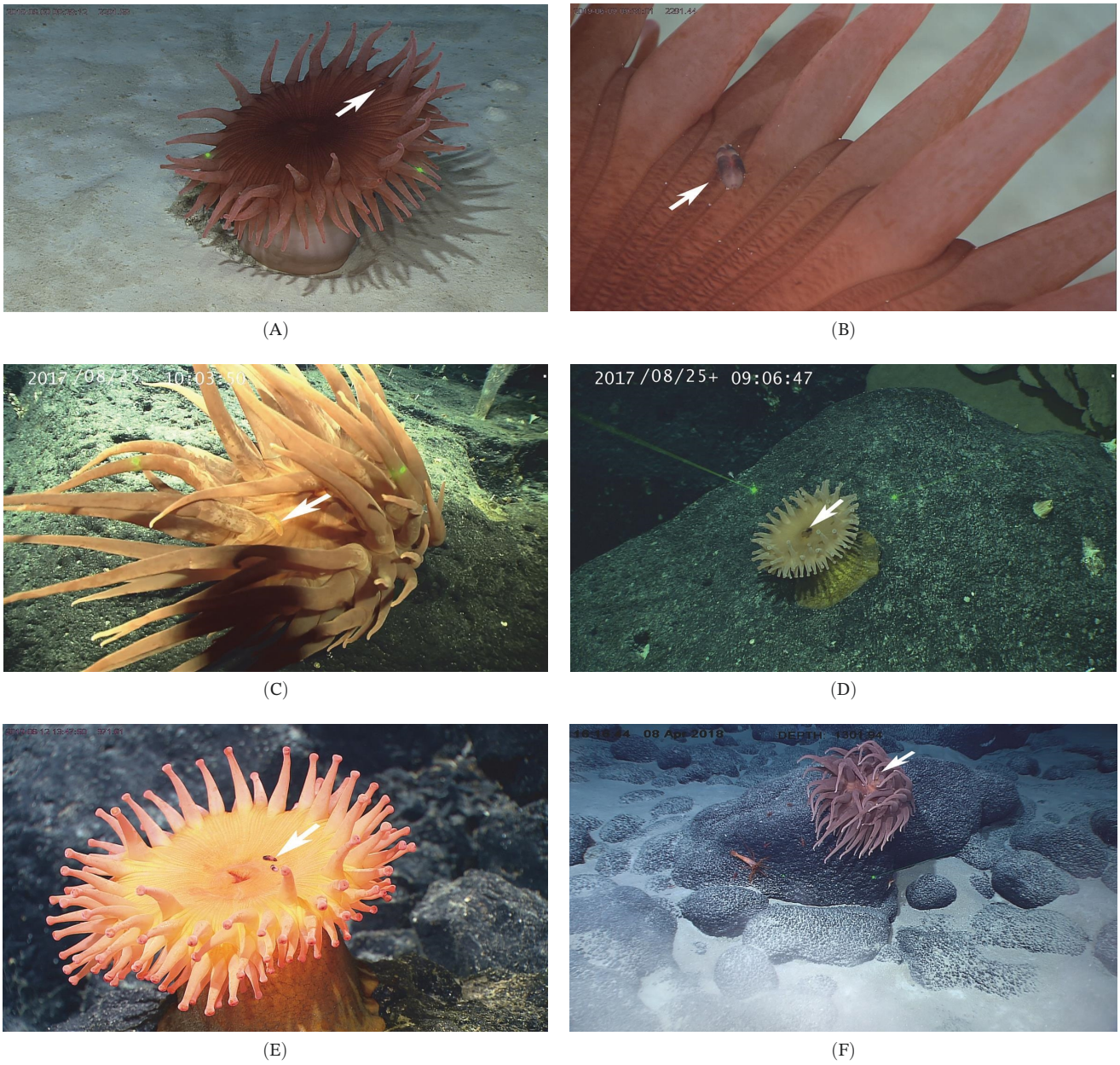


(A) (B) (C) (D) (E) (F)

**FIGURE 4** | In-situ photographs of symbiotic state between *Alentiana* specimens and their host anemones, arrow showing *Alentiana* specimens. (A, B) *A. barnichae* sp. nov., paratype (MBM286815), commensal with *Sicyonis* sp1.; (C) *A. barnichae* sp. nov., paratype (MBM287245), commensal with *Bolocera* sp.; (D) *A. fiegei* sp. nov., holotype (MBM287243), commensal with *Sicyonis* sp2.; (E) *A. fiegei* sp. nov., paratype (MBM287244), commensal with *Sicyonis* sp2.; (F) *A*. sp. (MBM287246), commensal with *Bolocera* sp.

1156 m, August 25, 2017; MBM286815, Dive 221, M5 seamount (140°08′52″E, 10°02′54″N), 2291 m, June 9, 2019.

**Etymology.** The specific epithet "barnichae" is a Latinized genitive honoring Dr. Ruth Barnich. It recognizes her significant contributions to polynoid taxonomy.

**Description.** Holotype (Figure 3A): well-preserved, 38 segments, length 38.50 mm, width 19.39 mm (incl. chaetae), 13.61 mm (excl. chaetae). Paratype: MBM287245 (Figures 3B, 4C), 39 segments (39th segment: left parapodium tiny, right parapodium absent), length 33.90 mm, width 15.30 mm (incl. chaetae) and 11.70 mm (excl. chaetae); MBM286815 (Figures 3C, 4A,B), 30 segments (posterior segments possibly regenerating; 30th segment: left parapodium tiny, right parapodium absent), length 7.24 mm, width 5.14 mm (incl. chaetae), 3.80 mm (excl. chaetae).

Body orange-yellow without distinct pigmentation (Figure 3A–C); oval shaped, slightly tapering posteriorly (Figures 5D, 6D, 7D); slightly arched dorsally, flattened ventrally. Following description mainly based on holotype.

Prostomium (Figures 5A, 6A, 7A) bilobed, wider than long. Median antenna (Figures 5A, 6A, 7A) with large and cylindrical ceratophore, inserted in anterior notch of prostomium; styles smooth, tapered, about two times length of lateral antennae. Lateral antennae (Figures 5A, 6A, 7A) inserted terminally on prostomium, with smaller and cylindrical ceratophores (than

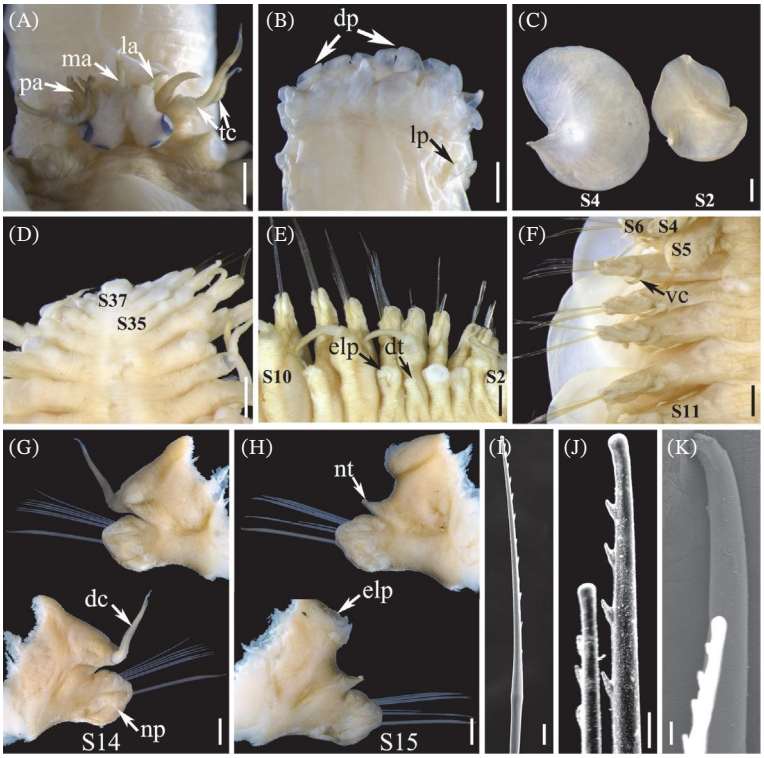


**FIGURE 5** | *Alentiana barnichae* sp. nov., holotype (MBM286814). (A) Head and anterior segments in dorsal view; (B) Extended pharynx in dorsal view; (C) Elytra of anterior segments; (D) Posterior segments in ventral view; (E) Left side of segments 2–10 in dorsal view; (F) Right side of segments 4–11 in ventral view; (G) Right parapodium on segment 14 in posterior (lower side) and anterior views (upper side); (H) Right parapodium on segment 15 in posterior (lower side) and anterior views (upper side); (I) Supraacicular chaeta; (J) Supraacicular chaeta, showing details of distal part; (K) Subacicular hooks. dc: dorsal cirrus; dp: distal papillae; dt: dorsal tubercles; elp: elytrophores; la: lateral antennae; lp: lateral papillae; ma: median antenna; np: neuropodia; nt: notopodia; pa: palp; S14: segment 14; tc: tentacular cirrus; vc: ventral cirrus. Scale bars: 1 mm (A–H), 50 μm (I), 20 μm (K), and 10 μm (J).

median ceratophore) formed by anterior prolongations of prostomial lobes; styles smooth, tapering distally to slender tips, shorter than prostomium. Two pairs of large, round, and dark eyes (Figures 5A, 6A, 7A), arranged as an inverted trapezoid; anterior pair larger than posterior pair, situated laterally on widest part of prostomium; posterior pair near hind margin of prostomium. Palps (Figures 5A, 7B) stout, much thicker than antennae, nearly as long as prostomium, tapered, smooth. Pharynx (Figure 5B) robust, with nine pairs of conical papillae located distally (nine dorsal, nine ventral), two pairs of lateral papillae located subterminally, and two pairs of usual polynoid jaws without teeth. First or tentacular segment (Figures 5A, 6A,B, 7A,B) achaetous, with two pairs of cylindrical tentaculophores inserted laterally to prostomium; dorsal tentacular cirri longer than ventral tentacular cirri, smooth, tapering distally to slender tips. Second segment (Figures 5A, 6A, 7A) with first pair of elytra, sub-biramous parapodia, and ventral cirri notably longer than subsequent ventral cirri.

Eighteen pairs of elytra attached to distinct inflated elytrophores (Figures 3A–C, 5E, 6E), arranged on segments 2, 4, 5, 7, 9, 11, 13, 15, 17, 19, 21, 23, 26, 29, 32, 35, 36, and 37 (Figure S4). Elytra (Figures 5C, 6C, 7C) oval to subreniform in shape, completely covering dorsum; pale, thick, without tubercles or papillae on margins or surfaces. Dorsal tubercles (Figures 3A–C, 5E) on cirrigerous segments, slightly nodular.

Parapodia (Figures 5G,H, 6G–I, 7E,F) elongated, almost as long as body width; flattened, sub-biramous throughout body. Dorsal cirri (Figures 5E,G, 6E,H, 7F) on cirrigerous segments, inserted on bulbous cirrophores, tapering distally to slender tips, not extending beyond neurochaetae. Notopodia (Figures 5H, 6G–I) reduced to a conical lobe with an embedded aciculum, without notochaetae. Neuropodia (Figures 5G, H, 6G–I, 7E,F) distally subtriangular, deeply notched dorsally and ventrally; prechaetal and postchaetal lobes similar in length, prechaetal lobe larger than postchaetal lobe in width, with lower margin overlaps that of postchaetal lobe. Neuropodia with two kinds of neurochaetae (Figures 5F–H, 6H,I, 7E,F), including six to 11 slender supraacicular chaetae and a heavy subacicular hook (rarely two in a parapodium). Supraacicular hook (Figures 5I, J, 6J,K, 7G) subdistally inflated, serrated on one side, distally bluntly rounded. Subacicular hooks (Figures 5K, 6J, 7G) subdistally inflated, distally falcate and smooth. Ventral cirri (Figures 5F, 6F,G,I, 7E,F) tapering, larger and thicker on segment 2, inserted basally on neuropodia; ventral cirri smaller on subsequent segments, inserted in middle of neuropodia. Ventral nephridial papillae (Figure 6F) small, beginning on segment 10.

**Type locality.** Tropical western Pacific, from seamounts M4 and M5.

**Variation.** *Alentiana barnichae* sp. nov. was represented by three specimens in this study, two of which were large, mature individuals with body lengths of 38.5 and 33.9 mm, respectively (Figure 3A,B). These two specimens exhibited highly congruent morphological traits. The third specimen (Figure 3C) was a small, underdeveloped individual (7.2 mm in body length). Significant

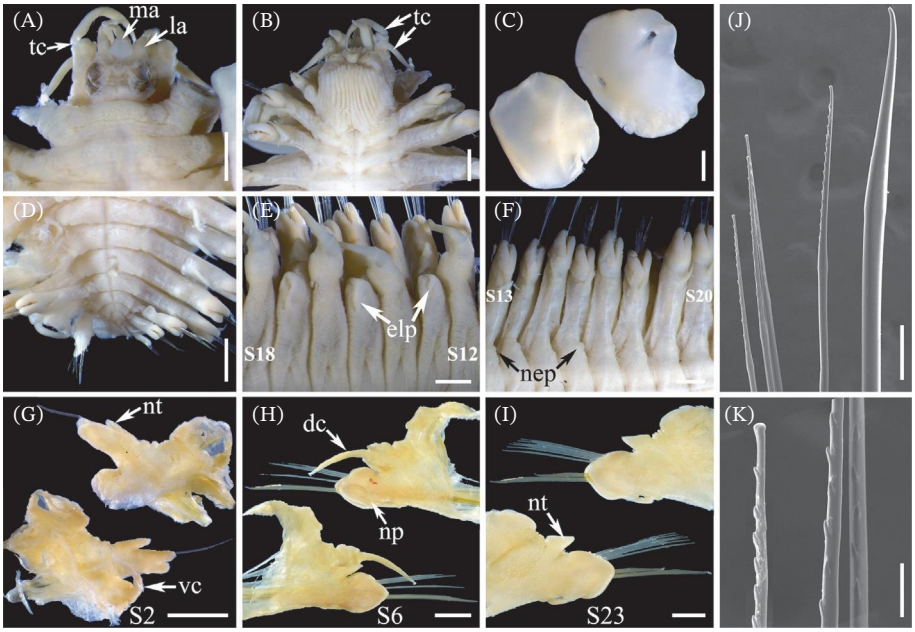


**FIGURE 6** | *Alentiana barnichae* sp. nov., paratype (MBM287245). (A) Head and anterior segments in dorsal view; (B) Head and anterior segments in ventral view; (C) Elytra; (D) Posterior segments in ventral view; (E) Left side of segments 12–18 in dorsal view; (F) Left side of segments 13–20 in ventral view; (G) Left parapodium on segment 2 in posterior (upper side) and anterior views (lower side); (H) Left parapodium on segment 6 in posterior (upper side) and anterior views (lower side); (I) Left parapodium on segment 23 in posterior (upper side) and anterior views (lower side); (J) Supraacicular chaetae and subacicular hook; (K) Supraacicular chaetae, showing details of distal part. dc: dorsal cirrus; elp: elytrophores; la: lateral antennae; ma: median antenna; np: neuropodia; nt: notopodia; S2: segment 2; tc: tentacular cirrus; vc: ventral cirrus. Scale bars: 1000 μm (A–I), 200 μm (J), and 50 μm (K).

morphological differences exist among individuals of different body sizes, mainly in body color, segment counts, elytral counts, elytral size, and neuropodial morphology.

First, notable body color differences were observed between large and small individuals. The body surfaces of the larger specimens are orange-yellow with no distinct pigmentation (Figure 3A,B), whereas the body surface of the smaller specimen, particularly the ventral trunk surface, neuropodia, and tips of the dorsoventral appendages (including the antennae, palps, tentacular cirri, dorsal cirri, and ventral cirri), bears black pigments (Figure 3C).

Second, the segment and elytral counts of the three specimens are positively correlated with body length: the two larger individuals (38.5 and 33.9 mm) possess 38/39 segments and 18 pairs of elytra, while the smaller individual (7.2 mm in body length) has 30 segments and 14 pairs of elytra. These meristic trait differences indicate typical ontogenetic variation rather than species-specific characteristics.

Third, elytral morphology differs markedly with body size. The elytra of the larger individuals are thicker, pale yellow in color, and lack distinct pigmentation (Figures 5C, 6C), whereas those of the smaller individual are thinner and cover a greater proportion of the dorsal body surface, bearing uniformly distributed black pigmentation (Figure 7C).

Fourth, neuropodial morphology shows clear ontogenetic variation. The neuropodia of the two large, mature specimens are broad and short, roughly triangular in shape, with an aspect ratio (length to width) of ~1:1 (Figures 5G,H, 6G–I). The prechaetal lobes are subequal in length to the postchaetal lobes. In contrast, the neuropodia of the smaller specimen are digitiform, with an aspect ratio of ~2.5:1 (Figure 7E,F). The prechaetal lobes are slightly larger than the postchaetal lobes, with their ventral margins slightly overlapping those of the postchaetal lobes.

Fifth, cephalic and dorsoventral appendages exhibit size-related morphological variation. The appendages (including the antennae, palps, tentacular cirri, and dorsal cirri) of the larger individuals are stout and short (Figures 5A, 6A). The antennae are shorter than the prostomium, and the dorsal cirri do not extend beyond the neurochaetae (Figures 5E, 6E). In contrast, the appendages of the smaller individual are relatively slender and elongated, with the antennae exceeding the prostomium in length (Figure 7A) and dorsal cirri clearly extending beyond the neurochaetae (Figure 7F).

Due to the significant ontogenetic variation mentioned above, species identification and interspecific comparisons should ideally be based on mature individuals with at least 35 segments and at least 16 pairs of elytra. At this stage, traits such as body color, neuropodial morphology, and elytral morphology are relatively stable. Accurate identification of immature individuals cannot be reliably achieved through morphological comparison alone, and COI gene sequence alignment is therefore recommended to verify species identity.

**Remarks.** *Alentiana barnichae* sp. nov. is recognized as a new species based on the presence of stable and clearly distinguishable morphological diagnostic characters from its congeneric relative *A. palinpoda*. Although the two species are similar in body size (*A. barnichae*: 33.9–38.5 mm in body length; *A. palinpoda*: 32 mm in body length) and share similar features such as head morphology, body maculation, or basic parapodial morphology, they differ strongly in key morphological traits: *A. barnichae* has distinct

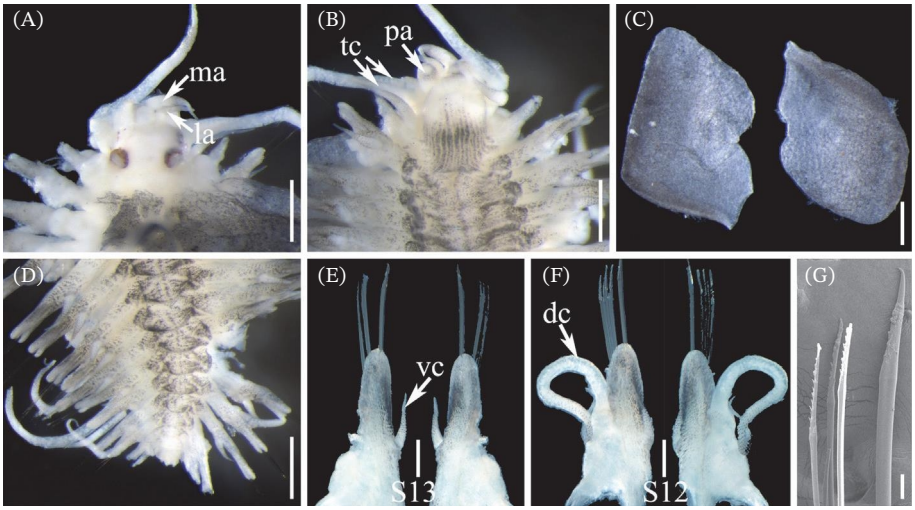


**FIGURE 7** | *Alentiana barnichae* sp. nov., paratype (MBM286815). (A) Head and anterior segments in dorsal view; (B) Head and anterior segments in ventral view; (C) Elytra of anterior segments; (D) Posterior segments in ventral view; (E) Left parapodium on segment 13 in posterior (right side) and anterior views (left side); (F) Left parapodium on segment 12 in posterior (right side) and anterior views (left side); (G) Supraacicular chaetae and subacicular hook. dc: dorsal cirrus; la: lateral antennae; ma: median antenna; pa: palp; S13: segment 13; tc: tentacular cirrus; vc: ventral cirrus. Scale bars: 500 μm (A–D), 100 μm (E, F), and 50 μm (G).

nodular dorsal tubercles, subtriangular neuropodia, and nephridial papillae starting from segment 10, whereas *A. palinpoda* has indistinct dorsal tubercles, nearly oval neuropodia, and nephridial papillae initiating from segment 4.

Two identification controversies exist when comparing the morphology of this species with *A. palinpoda*. First, the original description of *A. palinpoda* records 37 segments and 16 pairs of elytra extending to segment 35. However, our observations revealed that the terminal segments and elytra of *Alentiana* species are extremely delicate and thus easily overlooked, leading to counting biases that render these meristic traits poorly stable and unsuitable as core diagnostic criteria for distinguishing the two species. Second, the original description of *A. palinpoda* considers the "ventral curving upward and backward of the prechaetal lobe" as a key diagnostic feature of this species. However, detailed observations of the specimens in this study suggest that the lower margin of the prechaetal lobe naturally overlaps with that of the postchaetal lobe in *Alentiana* species, and this overlapping structure readily becomes curled during specimen preservation (Figure 5F). Therefore, the "curling trait" of the prechaetal lobe is not considered to be unique to *A. palinpoda* and thus cannot be used to distinguish *A. barnichae* from *A. palinpoda*.

*Alentiana barnichae* resembles *A. aurantiaca* in body size, segment number, and overall morphology. The primary morphological distinctions between the two species are as follows: (1) *A. barnichae* possesses 18 pairs of elytra, with the posteriormost pair located on segment 37 (Figure S4). By comparison, *A. aurantiaca* has up to 20 pairs of elytra, with the posteriormost pair extending to segment 39 [8]; (2) Nephridial papillae are absent or indistinct in *A. aurantiaca*, whereas conspicuous nephridial papillae are present in *A. barnichae*, first appearing on segment 10.

**GenBank accession numbers.** *Alentiana barnichae* sp. nov. (16S rRNA/COI): MBM286814 (PX938805/PX935556), MBM287245 (PX938806/PX935557), and MBM286815 (PX938804/PX935555).

### 3.3.3 | *Alentiana fiegei sp. nov.* (Figures 3, 4, 8, 9)

**Material examined.** Holotype: MBM287243, Dive 142, M4 seamount (140°10′54″E, 10°31′18″N), 1219.1 m, August 25, 2017. Paratype: MBM287244, Dive 224, M8 seamount (140°05′01″E, 10°36′55″N), 871 m, June 12, 2019.

**Etymology.** The specific epithet "fiegei" is a Latinized genitive honoring Dr. Dieter Fiege. It acknowledges his outstanding work on polynoid systematics.

**Description.** Holotype (Figures 3D, 4D): well-preserved, 31 segments, length 10.47 mm, width 6.95 mm (incl. chaetae), 5.33 mm (excl. chaetae). Paratype (Figures 3E, 4E): 23 segments (posterior segments regenerating; last two pairs of parapodia very small, poorly developed; Figure 9D,E), length 7.52 mm, width 5.75 mm (incl. chaetae), 4.40 mm (excl. chaetae).

Body (Figure 3D,E) oval shaped, slightly arched dorsally, flattened ventrally, tapering posteriorly (Figure 8E). Body pale with distinct dark pigments covered on tips of appendages (including antennae, palps, tentacular cirri, dorsal cirri and ventral cirri), neuropodia, and ventral surface of trunk (Figure 3D,E). Following description mainly based on holotype.

Prostomium (Figures 8A, 9A) bilobed, wider than long. Median antenna (Figures 8A, 9A,B) with cylindrical ceratophore, inserted in anterior notch of prostomium; styles tapered, about 1.5 times length of lateral antennae. Lateral antennae (Figures 8A, 9A,B) inserted terminally on prostomium, with smaller and cylindrical ceratophores formed by anterior prolongations of prostomial lobes; styles smooth, tapering distally to slender tips, nearly as long as prostomium. Two pairs of large, round, and dark eyes (Figures 8A, 9A), arranged as an inverted trapezoid; anterior pair larger than posterior pair, situated laterally on widest part of prostomium; posterior pair near hind margin of prostomium. Palps (Figures 8A, 9A,B) stout, much thicker than antennae, slightly longer than prostomium, tapered, smooth. Pharynx (Figure 8D) robust, with nine pairs of conical papillae located

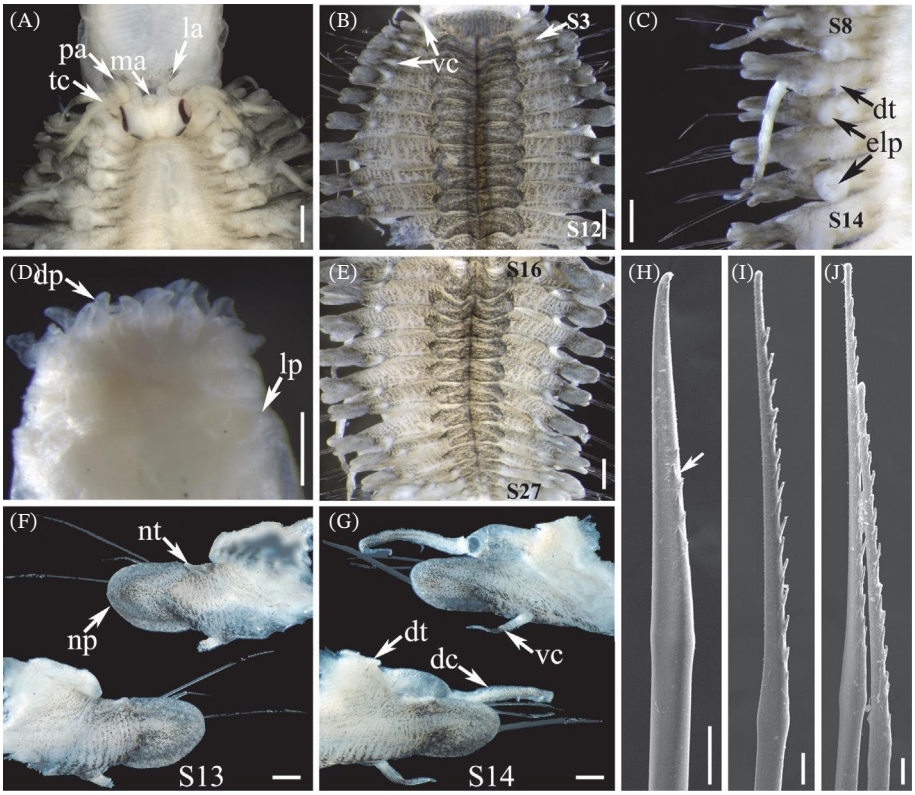


**FIGURE 8** | *Alentiana fiegei* sp. nov., holotype (MBM287243). (A) Head and anterior segments in dorsal view; (B) Anterior segments 2–12 in ventral view; (C) Left side of segments 8–14 in dorsal view; (D) Extended pharynx in dorsal view; (E) Posterior segments 15–27 in ventral view; (F) Left parapodium on segment 13 in posterior (upper side) and anterior views (lower side); (G) Left parapodium on segment 14 in posterior (upper side) and anterior views (lower side); (H) Subacicular hook, arrow showing spines of distal part; (I, J) Supraacicular chaetae. dc: dorsal cirrus; dp: distal papillae; dt: dorsal tubercles; elp: elytrophores; la: lateral antennae; lp: lateral papillae; ma: median antenna; np: neuropodia; nt: notopodia; pa: palp; S13: segment 13; tc: tentacular cirrus; vc: ventral cirrus. Scale bars: 500 μm (A–G), 50 μm (H), and 20 μm (I, J).

distally (nine dorsal, nine ventral), two pairs of lateral papillae located subterminally, and two pairs of usual polynoid jaws without teeth. First or tentacular segment (Figures 8A, B, 9A,B) achaetous, with two pairs of cylindrical tentaculophores inserted laterally to prostomium; dorsal tentacular cirri much longer than ventral tentacular cirri, smooth, tapering distally to slender tips. Second segment (Figures 8A,B, 9A,B) with first pair of elytra, subbiramous parapodia, and ventral cirri distinctly longer than subsequent ventral cirri.

Fourteen pairs of elytra attached to distinct inflated elytrophores (Figures 3D,E, 8A,C, 9A,D), arranged on segments 2, 4, 5, 7, 9, 11, 13, 15, 17, 19, 21, 23, 26, and 29. Elytra (Figure 9C) oval to subreniform in shape, completely covering dorsum; pale, soft, without tubercles or papillae on margins or surfaces. Dorsal tubercles (Figures 3D,E, 8C,G, 9A,G) on cirrigerous segments, slightly conical.

Parapodia (Figures 8F,G, 9G,H) elongated, as long as body width; flattened, sub-biramous throughout body. Dorsal cirri (Figures 8C,G, 9A,G) on cirrigerous segments, inserted on bulbous cirrophores, tapering distally to slender tips, not extending beyond neurochaetae. Notopodia (Figures 8F, 9H) reduced to a conical lobe with an embedded aciculum, without notochaetae. Neuropodia (Figures 8F,G, 9G,H) distally ovate, deeply notched dorsally and ventrally; prechaetal lobe slightly longer and wider than postchaetal lobe, with upper and lower margins overlapping those of postchaetal lobe. Neuropodia with two kinds of neurochaetae (Figures 8G, 9H), including five to 10 slender supraacicular chaetae and a heavy subacicular hook. Supraacicular hook (Figures 8I,J, 9J) subdistally inflated, serrated on one side, distally bluntly pointed. Subacicular hooks (Figures 8H, 9I) subdistally inflated, distally falcate, with 4–6 spines on inner surface. Ventral cirri (Figures 8E–G, 9F–H) tapering, longer and thicker on segment 2, inserted basally on neuropodia; ventral cirri smaller on subsequent segments, inserted in middle of neuropodia. Ventral nephridial (Figures 8B,E, 9E,F) papillae indistinct.

**Type locality.** Tropical western Pacific, from seamounts M4 and M8.

**Variation.** This study included two similar-sized subadult specimens of *Alentiana fiegei* sp. nov.: the larger individual (10.47 mm in body length) had 31 body segments and 14 pairs of elytra; the smaller specimen (7.52 mm in body length) had only 23 observable segments, due to initial regeneration following posterior body fragmentation and underdevelopment of the regenerating segments.

Due to their similar body sizes, no significant differences were observed between the two specimens in head morphology, body surface maculation or basic parapodial morphology. The primary

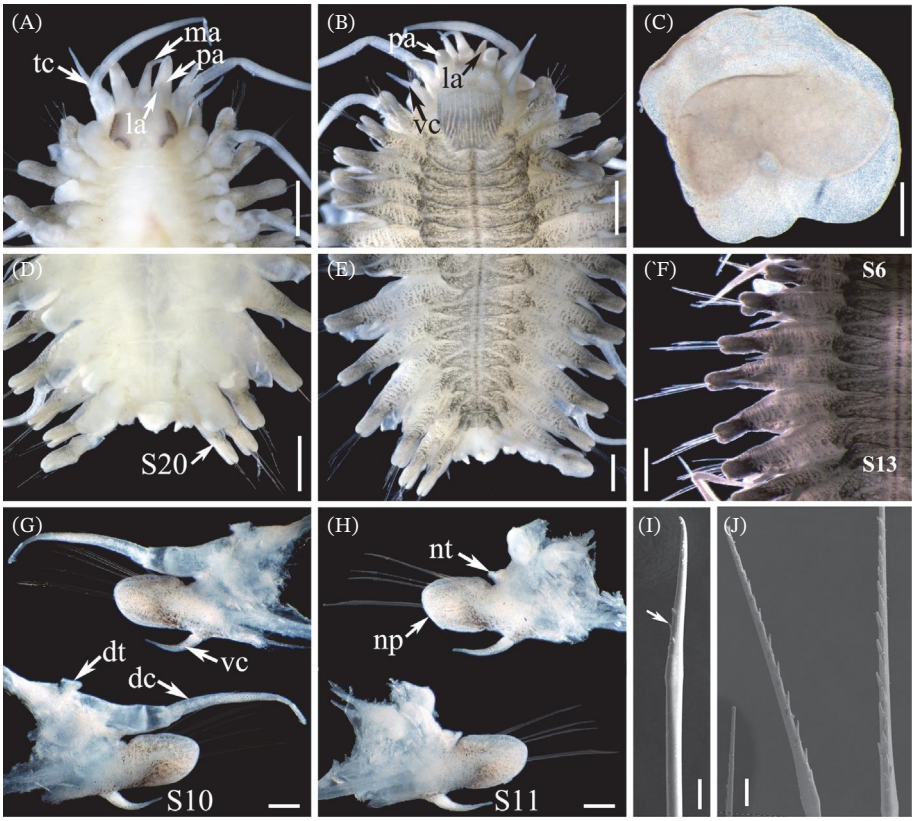


**FIGURE 9** | *Alentiana fiegei* sp. nov., paratype (MBM287244). (A) Head and anterior segments in dorsal view; (B) Head and anterior segments in ventral view; (C) Elytra; (D) Posterior segments in dorsal view; (E) Posterior segments in ventral view; (F) Right side of segments 6–13 in ventral view; (G) Left parapodium on segment 10 in posterior (upper side) and anterior views (lower side); (H) Left parapodium on segment 11 in posterior (upper side) and anterior views (lower side); (I) Subacicular hook, arrow showing spines of distal part; (J) Supraacicular chaetae. dc: dorsal cirrus; dt: dorsal tubercles; la: lateral antennae; ma: median antenna; np: neuropodia; nt: notopodia; pa: palp; S10: segment 10; tc: tentacular cirrus; vc: ventral cirrus. Scale bars: 500 μm (A–H), 50 μm (I), and 20 μm (J).

difference lay in the morphology of dorsal cirri: those of the smaller individual were relatively longer and more slender, significantly exceeding the neurochaetae in length (Figure 9G). In contrast, dorsal cirri of the larger specimen were shorter and stouter, not extending beyond the neurochaetae (Figure 8G).

**Remarks.** *Alentiana fiegei* sp. nov. is represented by immature subadult specimens in this study. Meristic traits including segment and elytral counts are closely linked to developmental stage, resulting in fewer segments and elytra in this species than in fully mature congeneric individuals. Accordingly, these counts are not appropriate as primary taxonomic diagnostic traits for *A. fiegei*.

In other morphological traits, *A. fiegei* sp. nov. is most closely allied to *A. barnichae* sp. nov., sharing high congruence in key characters including head morphology, pharyngeal structure, and body surface maculation. However, the two species can be readily distinguished by two stable diagnostic traits. First, the subacicular hook of *A. fiegei* bears 4–6 small spines near its distal end, while that of *A. barnichae* is smooth and lacks any spines. Second, *A. fiegei* entirely lacks distinct nephridial papillae, whereas *A. barnichae* possesses well-developed nephridial papillae originating from segment 10 and extending posteriorly along the body.

**GenBank accession numbers.** *Alentiana fiegei* sp. nov. (16S rRNA/COI): MBM287243 (PX938807/PX935558) and MBM287244 (PX938808/PX935559).

## 4 | Discussion

### 4.1 | Species Diversity and Geographical Distribution of the Genus *Alentiana*

Two new species of the genus *Alentiana* are described herein from four seamounts in the tropical western Pacific, thereby increasing the total number of valid species in the genus to four. Among these, three species, namely *Alentiana palinpoda*, *A. barnichae*, and *A. fiegei*, are distributed on seamounts in the western Pacific ([9]; this study), whereas the fourth species, *A. aurantiaca*, is restricted to the western North Atlantic [6, 8]. A putative *Alentiana* record from European waters [10] is regarded as unconfirmed and probably represents a misidentification, according to taxonomic remarks by Barnich [49]. Despite the formal recognition of four valid species, the actual species diversity of *Alentiana* remains insufficiently explored. For instance, the National Oceanic and Atmospheric Administration (NOAA) has recorded high-definition images of *Alentiana* individuals inhabiting the tentacles or oral discs of sea anemones during investigations of the Northwestern Hawaiian Ridge and adjacent seamounts. These records suggest that further undescribed species may exist within the genus. Future studies should therefore implement targeted deep-sea sampling and integrated taxonomic research combining morphological and molecular evidence.

The geographical distribution of the genus is closely associated with the distributions of its deep-sea sea anemone hosts. To date, the genus is known to be distributed in the Pacific and Atlantic Oceans. However, deep-sea sea anemone hosts represented by *Bolocera* Gosse, 1860 [50] are widely distributed throughout all major oceans worldwide [51, 52]. Accordingly, *Alentiana* is inferred to have the potential for widespread occurrence in other deep-sea regions globally.

### 4.2 | Symbiotic Traits and Host Range Expansion of *Alentiana*

Polynoidae exhibit a broad host range, encompassing cnidarians, decapod crustaceans, echinoderms, mollusks, polychaetes, and sponges (e.g., [2, 9, 53–67]). Among these hosts, cnidarians display the highest diversity, predominantly including skeleton-bearing groups such as Scleractinia Bourne, 1900 [68] (stony corals), Alcyonacea Lamouroux, 1812 [69] (soft corals), and Hydrozoa Owen, 1843 [70] (hydroids) [71]. In contrast, reports of polynoids forming symbioses with skeleton-less sea anemones (Actiniaria Hertwig, 1882 [72]) are extremely rare [8, 73], and *Alentiana* is currently the only known polynoid genus that is obligately symbiotic with actiniarians, typically living commensally among the tentacles of large sea anemones.

Prior to the present study, only three cases of symbiosis between polynoids and actiniarians had been documented: Molodtsova et al. [71] reported *Alentiana aurantiaca* symbiotic with the giant sea anemone *Bolocera tuediae* (Johnston, 1832) [74], and *Arctonoe vittata* (Grube, 1855) [75] in association with *Metridium senile* (Linnaeus, 1761) [76]. Additionally, *Alentiana palinpoda* was documented in association with an unidentified large sea anemone of the family Actiniidae Rafinesque, 1815 [77], presumably a species of *Bolocera* [9]. The present study further expands the symbiotic range between polynoids and sea anemones: *Alentiana* species not only form symbioses with large *Bolocera* species but also with two additional sea anemones of the genus *Sicyonis* Hertwig, 1882 [72] (Table 1; Figure 4).

Furthermore, the present study confirms that *Alentiana* is not a monoxenous (single-host) symbiont as previously proposed [2], but rather a polyxenous (multiple-host) genus, meaning that a single species can establish symbiotic relationships with different sea anemone hosts. To date, no published studies have investigated the host selection mechanisms or host-switching strategies of *Alentiana* among different sea anemone species, and this scientific question merits further in-depth investigation in future studies.

### 4.3 | Morphological Variation in *Alentiana* and Its Taxonomic Implications

As segment and elytral counts are relatively stable taxonomically in most Polynoidae genera, they are considered core diagnostic characters for the family [12, 14, 18, 78, 79]. However, the taxonomic utility of these traits in *Alentiana* is severely limited by three key factors. First, these meristic traits exhibit typical ontogenetic variation, displaying a distinct positive correlation with body length. Second, the diameter of terminal segments in *Alentiana* specimens decreases sharply from the 34th segment onward, and elytra are prone to detachment during sampling and preservation. This directly reduces the accuracy of counting and has led to inconsistencies in early taxonomic descriptions of the genus. Third, posterior fragmentation and regeneration further interfere with counting accuracy. This study is the first to document posterior regeneration in *Alentiana*. Regenerated segments are slimmer, with incompletely developed structures (e.g., elytra and parapodia). Paratypes of *A. fiegei* and *A. barnichae* both show signs of posterior regeneration, resulting in distinct discrepancies between the countable and original segment counts of the individuals.

Elytral morphological traits, including size, color, and thickness, also exhibit significant intraspecific variation in *Alentiana*. For instance, the elytral morphology of *A. aurantiaca* has been inconsistently described in various studies. Hartman [6] described the elytra as "pale, thick… leaving the median dorsum broadly exposed," whereas Pettibone [8] documented the elytra of the same species as "large, reniform, overlapping, covering the dorsum… thin, soft, translucent." Observations of *A. barnichae* in the present study further supplement the pattern of intraspecific elytral variation within this genus: larger individuals have thick, pale-yellow elytra with no distinct pigmentation, whereas smaller individuals have thinner elytra that cover a larger dorsal area and bear black pigmentation on their surfaces. These variations are associated with the ontogenetic stage of the individuals and are not interspecific diagnostic traits.

Neuropodial morphology in *Alentiana* exhibits ontogenetic variation associated with individual body size. In this genus, neuropodia are predominantly triangular or oval in larger individuals but digitiform in smaller ones, and this morphological difference is not a species-specific trait. For example, in *A. barnichae*, individuals with a body length exceeding 30 mm have subtriangular neuropodia with an approximate aspect ratio (length: width) of 1:1, while those with a body length less than 10 mm have digitiform neuropodia with an aspect ratio of ~2.5:1. This highlights the need to fully consider individual body size when using neuropodial morphological traits for taxonomic comparisons of this genus.

In summary, the classical traits traditionally used for species-level identification in the Polynoidae, including segment and elytral counts and morphology, as well as neuropodial morphology, either exhibit obvious variation or are difficult to quantify accurately in *Alentiana*. This poses greater technical challenges for species description and identification within this genus. Therefore, future taxonomic studies of *Alentiana* should incorporate more stable diagnostic characters (e.g., chaetal features, nephridial papilla morphology) and molecular data, and species identification and interspecific comparisons should ideally be based on mature individuals (≥35 segments, ≥16 pairs of elytra) which have relatively stable key traits (e.g., body color, neuropodial, and elytral morphology). This will ensure the accuracy and consistency of the taxonomic identification for *Alentiana* species.

### 4.4 | Systematics and Phylogeny of *Alentiana* and Related Groups

In this study, genome skimming was employed to generate the mitochondrial genomes and ribosomal gene sequences of *Alentiana* species. Combined with Polynoidae gene sequences retrieved from GenBank, the first comprehensive phylogenetic analysis of

this genus was performed. The results support the monophyly of the genus *Alentiana* and revealed its close phylogenetic affinity with the subfamily Macellicephalinae. Our phylogenetic analysis also reveals the polyphyly of the subfamily Lepidastheniinae, highlighting the need for a comprehensive phylogenetic analysis of all genera within this subfamily and a corresponding revision of its taxonomy. However, due to the limited availability of samples and genetic data, this study was unable to conduct a comprehensive taxonomic revision of Lepidastheniinae. Although *Alentiana* forms a sister group with Macellicephalinae, the two lineages exhibit significant morphological differences. Therefore, this study does not recommend assigning *Alentiana* to Macellicephalinae, and retains its placement within Lepidastheniinae. Pending the taxonomic revision of Lepidastheniinae, this study also does not support the establishment of a distinct new subfamily for *Alentiana*.

The monophyly of the subfamily Lepidonotinae is also not supported, with clear inconsistencies between the phylogenetic *positions and current taxonomic placements of some species: Hyperhalosydna striata*, originally placed in Lepidastheniinae, nests within the core clade of Lepidonotinae. *We suggest that taxonomic revision or generic transfer of Hyperhalosydna should be carried out based on* resequencing of reliable specimens and morphological verification of voucher specimens associated with published sequences, under an integrative taxonomic framework combining morphological and molecular evidence. Whereas *Alentia gelatinosa*, formally assigned to Lepidonotinae, falls outside the Lepidonotinae core clade and clusters with *Eulagiscagigantea* (Eulagiscinae). This anomalous phylogenetic placement is consistent with its long-controversial taxonomic status: *Alentia gelatinosa* has undergone multiple taxonomic revisions since its original description, first described as *Polynoe gelatinosa* and subsequently transferred to the genera *Halosydna* Kinberg, 1856 and Alentia sequentially. Morphologically, this species differs substantially from other Lepidonotinae genera in key diagnostic traits, including the insertion position of lateral antennae and segment count. This further suggests the inaccuracy of its current taxonomic placement. Accordingly, Wu et al. [80] proposed assigning it to Polynoidae incertae sedis.

The subfamily Lepidastheniinae was originally split from Lepidonotinae. The two subfamilies have long been considered closely related due to their shared morphological character: terminally inserted lateral antennae. However, the phylogenetic results of this study demonstrate no close phylogenetic relationship between the two subfamilies. Future phylogenetic studies should therefore broaden taxon sampling and generate more comprehensive genetic data to better resolve the phylogenetic relationships within and between these two subfamilies, thereby facilitating a robust revision of their taxonomic delimitations.

### 4.5 | Character Evolution of Key Morphological Traits in Polynoidae

The presence or absence of lateral antennae, as well as their insertion position, constitutes core diagnostic characters for the classification of subfamilies and genera within the family Polynoidae (e.g., [81, 82]). Ancestral character state reconstruction performed herein reveals that terminally or subterminally inserted lateral antennae represent a plesiomorphic state for Polynoidae, a trait not exclusive to the subfamilies Lepidastheniinae and Lepidonotinae. Specifically, the subfamily Admetellinae possesses terminally inserted lateral antennae, whereas the subfamily Eulagiscinae and the species *Alentia gelatinosa* exhibit subterminally inserted ones. Given their high morphological similarity, ambiguous boundaries, and propensity for taxonomic confusion, these two character states were treated as a single character in the present evolutionary analysis. This constitutes the primary reason that the two subfamilies lack the close phylogenetic affinity previously assumed: the shared plesiomorphy of terminally or subterminally inserted lateral antennae does not reflect an exclusive phylogenetic relationship and thus cannot serve as valid taxonomic evidence to support their close affinities.

Furthermore, ventrally and terminoventrally inserted lateral antennae were also treated as a single character due to their morphological similarity and indistinct boundaries. Polynoinae (characterized by ventrally inserted lateral antennae) and Arctonoinae (characterized by terminoventrally inserted antennae) form a sister clade. This phylogenetic relationship further corroborates the close evolutionary connection between these two insertion modes. Ventrally or terminoventrally inserted lateral antennae represent a synapomorphy for the clade consisting of these two subfamilies, whereas the absence of lateral antennae constitutes a unique synapomorphy of the subfamily Macellicephalinae. Notably, both synapomorphies are derived from the plesiomorphic state of terminally inserted lateral antennae.

Deeply incised neuropodia have long been considered one of the diagnostic characters of Lepidastheniinae, together with terminally inserted antennae and other features employed by Pettibone [5] to define this subfamily and separate it from Lepidonotinae. However, ancestral character state reconstruction herein indicates that dorsoventrally deeply incised neuropodia are not unique to Lepidastheniinae, but instead arose via convergent evolution. In fact, parapodial traits are prone to convergent evolution under ecological pressures, a pattern also documented in other annelid lineages. In these lineages, similar neuropodial structures may evolve independently under analogous ecological pressures [4, 83]. A representative example is the genus Branchipolynoe (Macellicephalinae): species of this genus are symbiotic with deep-sea mussels in chemosynthetic habitats including hydrothermal vents and cold seeps, and their specialized habitat is likely the driver underlying the evolution of deeply incised neuropodia. This indicates that this trait cannot be used as an exclusive diagnostic character to define Lepidastheniinae. Additionally, the scattered placement of representative species of Lepidastheniinae across the phylogenetic tree further suggests that deeply incised neuropodia cannot be considered a synapomorphy for this subfamily. This finding provides morphological evolutionary evidence for the polyphyly of Lepidastheniinae, and also highlights the limitations of defining subfamilies based solely on a single morphological trait.

**Acknowledgments**

We sincerely thank the crew of R/V KeXue and the ROV FaXian for their valuable assistance in sample collection. We are grateful to Dr. Yang Li for identifying the sea anemones associated with the examined material.

We also thank Dr. Yuanyuan Sun for her kind assistance with scanning electron microscopy (SEM) operations.

### Funding

This research was funded by the Independent Deployment Project of the Institute of Oceanology, Chinese Academy of Sciences, Grant number IOCASZZZX301; the Natural Science Foundation of Shandong Province, China, Grant number ZR2025MS691; and the Biological Resources Programme, Chinese Academy of Sciences, Grant number CAS-TAX-24-033.

### Conflicts of Interest

The authors declare no conflicts of interest.

### Data Availability Statement

The materials described in this study are available at the Marine Biological Museum of Chinese Academy of Sciences (MBMCAS) at Institute of Oceanology, Qingdao, China. Voucher IDs: *Alentiana barnichae* sp. nov., MBM286814, MBM286815, and MBM287245; *A. fiegei* sp. nov., MBM287243 and MBM287244. The WGS data that support the findings of this study have been deposited in NCBI SRA GenBank (Table 2). The registration of *Alentiana barnichae* and *A. fiegei* in Zoobank are as follows: urn:lsid:zoobank.org:act:C7430A0F-B004-4AE5-993B-EDB559F2725E, and urn:lsid:zoobank.org:act:D0088DDD-3CCB-4286-AE98-FB6A17513293. The publication LSID: urn:lsid:zoobank.org:pub:D7763137-D883-400E-A463-21199FEE5F46.

### References

1. J. G. H. Kinberg, "Nya slägten och arter af Annelider. Öfversigt af Kongl," *Vetenskaps-Akademiens Förhhandlingar Stockholm* 12, no. 9-10 (1856): 381–388.

2. D. Martin and T. A. Britayev, "Symbiotic Polychaetes Revisited: An Update of the Known Species and Relationships (1998-2017)," *Oceanography and Marine Biology: An Annual Review* 56 (2018): 371–447.

3. S. Hourdez, B. C. Gonzalez, and D. Eibye-Jacobsen, "Aphroditiformia," in *Handbook of Zoology: Pleistoannelida, Errantia II, Phyllodocida*, eds. G. Purschke, M. Böggemann, and W. Westheide, (De Gruyter GmbH & Co. KG, 2022): 65–73.

4. G. W. Rouse, F. Pleijel, and E. Tilic, *Annelida* (Oxford University Press, 2022).

5. M. H. Pettibone, "A New Species of *Benhamipolynoe* (Polychaeta: Polynoidae: Lepidastheniinae) From Australia, Associated With the Unattached Stylasterid Coral *Conopora adeta*," *Proceedings of the Biological Society of Washington* 102, no. 2 (1989): 300–304.

6. O. Hartman, "A Review of the Types of Polychaetous Annelids at the Peabody Museum of Natural History, Yale University," *Bulletin of the Bingham Oceanographic Collection* 8 (1942): 1–98.

7. A. E. Verrill, "Notice of Recent Additions to the Marine Invertebrata of the Northeastern Coast of America, With Descriptions of New Genera and Species and Critical Remarks on Others," *Proceedings of the United States National Museum* 8, no. 534 (1885): 424–448.

8. M. H. Pettibone, "Marine Polychaete Worms of the New England Region, 1. Families Aphroditidae Through Trochochaetidae," *United States National Museum Bulletin* 227 (1963): 1–356.

9. Y. Wang, H. Cheng, and C. Wang, "*Alentiana palinpoda*, a New Commensal Polynoid Species From a Seamount in the Northwest Pacific Ocean," *Acta Oceanologica Sinica* 40, no. 12 (2021): 12–19.

10. L. Amoureux, G. Josef, and B. O'Connor, "Annélides Polychètes De l'éponge *Fasciospongia cavernosa* Schmidt," *Cahiers De Biologie Marine* 21 (1980): 387–392.

11. G. Read and K. Fauchald, "World Polychaeta Database. *Alentiana aurantiaca* (Verrill, 1885). World Register of Marine Species," 2026, https://www.marinespecies.org/aphia.php?p=taxdetails&id=130723.

12. R. Barnich and D. Fiege, "The Aphroditoidea (Annelida, Polychaeta) of the Mediterranean Sea," *Abhandlungen der Senckenbergischen Naturforschenden Gesellschaft* 559 (2003): 1–167.

13. R. Barnich and D. Fiege, "Revision of the Genus, *Lepidastheniella*, Monro, 1924 (Polychaeta: Polynoidae: Lepidastheniinae) With Notes on the Subfamily Lepidastheniinae and the Description of a New Species," *Journal of Natural History* 38, no. 7 (2004): 863–876.

14. T. Wehe, "Revision of the Scale Worms (Polychaeta: Aphroditoidea) Occurring in the Seas Surrounding the Arabian Peninsula, 1," *Polynoidae. Fauna of Arabia* 22 (2006): 23–197.

15. P. Salazar-Silva, "Scaleworms (Polychaeta: Polynoidae) From the Mexican Pacific and Some Other Eastern Pacific Sites," *Investigaciones Marinas* 34, no. 2 (2006): 143–161.

16. S. I. Salazar-Vallejo, N. E. González, and P. Salazar-Silva, "*Lepidasthenia loboi* Sp. n. From Puerto Madryn, Argentina (Polychaeta, Polynoidae)," *ZooKeys* 546 (2015): 21–37.

17. Y. Zhang, J. Sun, G. W. Rouse, et al., "Phylogeny, Evolution and Mitochondrial Gene Order Rearrangement in Scale Worms (Aphroditiformia, Annelida)," *Molecular Phylogenetics and Evolution* 125 (2018): 220–231.

18. P. Bonifácio and L. Menot, "New Genera and Species From the Equatorial Pacific Provide Phylogenetic Insights Into Deep-Sea Polynoidae (Annelida)," *Zoological Journal of the Linnean Society* 185, no. 3 (2019): 555–635.

19. A. S. Hiley, N. Mongiardino Koch, and G. W. Rouse, "Phylogenetics of Lepidonotopodini (Macellicephalinae, Polynoidae, Annelida) and Comparative Mitogenomics of Shallow-Water vs. Deep-Sea Scaleworms (Aphroditiformia)." *Biology* 13, no. 12 (2024): 979.

20. A. S. Hiley, K. R. Green, and G. W. Rouse, "Seven New Species of Scaleworms (Lepidonotopodini, Polynoidae, Polychaeta, Annelida) From Deep-Sea Chemosynthetic-Based Ecosystems," *Marine Biodiversity* 55, no. 6 (2025): 1–42, 2025, https://link.springer.com/article/10.1007/s12526-025-01580-7.

21. A. M. Bolger, M. Lohse, and B. Usadel, "Trimmomatic: A Flexible Trimmer for Illumina Sequence Data," *Bioinformatics* 30, no. 15 (2014): 2114–2120.

22. D. Li, C. M. Liu, R. Luo, K. Sadakane, and T. W. Lam, "MEGAHIT: An Ultra-Fast Single-Node Solution for Large and Complex Metagenomics Assembly via Succinct de Bruijn Graph," *Bioinformatics* 31, no. 10 (2015): 1674–1676.

23. C. Camacho, G. Coulouris, V. Avagyan, et al., "BLAST+: Architecture and Applications," *BMC Bioinformatics* 10, no. 1 (2009): 412.

24. R. Rose, O. Golosova, D. Sukhomlinov, A. Tiunov, and M. Prosperi, "Flexible Design of Multiple Metagenomics Classification Pipelines With UGENE," *Bioinformatics* 35, no. 11 (2019): 1963–1965.

25. K. Tamura, G. Stecher, D. Peterson, A. Filipski, and S. Kumar, "MEGA6: Molecular Evolutionary Genetics Analysis Version 6.0," *Molecular Biology and Evolution* 30, no. 12 (2013): 2725–2729.

26. G. M. R. Levinsen, "Systematisk-Geografisk Oversigt Over de Nordiske Annulata, Gephyrea, Chaetognathi Og Balanoglossi," *Videnskabelige Meddelelser fra Dansk Naturhistorisk Forening i Köbenhavn* 1882 (1883): 160–251.

27. A. E. Grube, *Actinien, Echinodermen Und Würmer Des Adriatischen-Und Mittelmeers Nach Eigenen Sammlungen Beschrieben* (J. H. Bon, 1840).

28. F. Sievers and D. G. Higgins, "Clustal Omega for Making Accurate Alignments of Many Protein Sequences," *Protein Science* 27, no. 1 (2018): 135–145.

29. J. Castresana, "Selection of Conserved Blocks From Multiple Alignments for Their Use in Phylogenetic Analysis," *Molecular Biology and Evolution* 17, no. 4 (2000): 540–552.

30. G. Vaidya, D. J. Lohman, and R. Meier, "SequenceMatrix: Concatenation Software for the Fast Assembly of Multi-Gene Datasets With Character Set and Codon Information," *Cladistics* 27, no. 2 (2011): 171–180.

31. S. Kalyaanamoorthy, B. Q. Minh, T. K. F. Wong, A. von Haeseler, and L. S. Jermiin, "ModelFinder: Fast Model Selection for Accurate Phylogenetic Estimates," *Nature Methods* 14, no. 6 (2017): 587–589.

32. B. Q. Minh, H. A. Schmidt, O. Chernomor, et al., "IQ-TREE. 2: New Models and Efficient Methods for Phylogenetic Inference in the Genomic Era," *Molecular Biology and Evolution* 37, no. 5 (2020): 1530–1534.

33. S. Guindon, J. F. Dufayard, V. Lefort, M. Anisimova, W. Hordijk, and O. Gascuel, "New Algorithms and Methods to Estimate Maximum-Likelihood Phylogenies: Assessing the Performance of PhyML 3.0," *Systematic Biology* 59, no. 3 (2010): 307–321.

34. D. T. Hoang, O. Chernomor, A. von Haeseler, B. Q. Minh, and L. S. Vinh, "UFBoot2: Improving the Ultrafast Bootstrap Approximation," *Molecular Biology and Evolution* 35, no. 2 (2018): 518–522.

35. F. Ronquist, M. Teslenko, P. van der Mark, et al., "MrBayes 3.2: Efficient Bayesian Phylogenetic Inference and Model Choice Across a Large Model Space," *Systematic Biology* 61, no. 3 (2012): 539–542.

36. A. Rambaut, A. J. Drummond, D. Xie, G. Baele, and M. A. Suchard, "Posterior Summarization in Bayesian Phylogenetics Using Tracer 1.7," *Systematic Biology* 67, no. 5 (2018): 901–904.

37. A. Rambaut, "FigTree 1.4.3," 2016, http://tree.bio.ed.ac.uk/software/figtree/.

38. L. J. Revell, "Phytools: An R Package for Phylogenetic Comparative Biology (and Other Things)," *Methods in Ecology and Evolution* 3, no. 2 (2012): 217–223.

39. G. Hartmann-Schröder, "Annelida, Borstenwürmer, Polychaeta," in *Tierwelt Deutschlands Und Der Angrenzenden Meeresteile Nach Ihren Merkmalen Und Nach Ihrer Lebensweise*, eds. M. Dahl and F. Peus, no. 58, (Gustav Fischer Verlag, 1971): 1–594.

40. J. R. Hanley, "Revision of the Scaleworm Genera, *Arctonoe*, Chamberlin and, *Gastrolepidia*, Schmarda (Polychaeta: Polynoidae) With the Erection of a New Subfamily Arctonoinae," *The Beagle: Records of the Museums and Art Galleries of the Northern Territory* 6, no. 1 (1989): 1–34.

41. A. Willey, "XII. Polychaeta," in *Report on the Collections of Natural History Made in the Antarctic Regions During the Voyage of the "Southern Cross*, eds. B. Sharpe and J. Bell, (British Museum, 1902): 262–283.

42. M. Sars, "Beskrivelser Og Iagttagelser over Nogle Moerkelige Eller Nye i Havet Ved Den Bergenske Kyst Levende Dyr Af Polypernes, Acalephernes, Radiaternes, Annelidernes Og Molluskernes Classer, Med en Kort Oversigt over De Hidtil Af Forfatteren Sammesteds Fundne Arter Og Deres Forekommen," in *Thorstein Hallagers Forlag Hos Chr*, (1835).

43. C. C. A. Monro, "Polychaeta. B.A.N.Z," *Antarctic Research Expedition Reports, Ser. B Zoology and Botany* 4, no. 4 (1939): 87–156.

44. M. H. Pettibone, "Revision of the Scaleworm Genus, *Eulagisca*, McIntosh (Polychaeta: Polynoidae) With the Erection of the Subfamily Eulagiscinae and the New Genus *Pareulagisca*," *Proceedings of the Biological Society of Washington* 110, no. 4 (1997): 537–551.

45. P. V. Uschakov, "Phylogenetic Relationships in the Family Polynoidae (Polychaeta)," in *Essays on Polychaetous Annelids in Memory of Dr. Olga Hartman*, eds. D. J. Reish and K. Fauchald, (University of Southern California, Allan Hancock Press, 1977): 29–38.

46. M. H. Pettibone, "A New Scale-Worm Commensal With Deep-Sea Mussels on the Galapagos Hydrothermal Vent (Polychaeta: Polynoidae)," *Proceedings of the Biological Society of Washington* 97, no. 1 (1984): 226–239.

47. A. E. Grube, "Die Familien der Anneliden," *Archiv für Naturgeschichte* 16, no. 1 (1850): 249–364.

48. R. P. Dales, "The Polychaete Stomodeum and the Inter-Relationships of the Families of Polychaeta," *Proceedings of the Zoological Society of London* 139, no. 3 (1962): 389–428.

49. G. Read and K. Fauchald, "World Polychaeta Database. Lepidastheniinae Pettibone," 2026, https://www.marinespecies.org/aphia.php?p=taxdetails&id=237617 World Register of Marine Species at: 1989.

50. P. H. Gosse, *Actinologia Britannica. A History of the British Sea-Anemones and Corals*, (1860).

51. D. G. Fautin, T. Zelenchuk, and D. Raveendran, "Genera of Orders Actiniaria and Corallimorpharia (Cnidaria, Anthozoa, Hexacorallia), and Their Type Species," *Zootaxa* 1668, no. 1 (2007): 183–244.

52. E. Rodríguez, D. Fautin, and M. Daly, "World List of Actiniaria. *Bolocera*, Gosse, 1860," 2026, World Register of Marine Species https://www.marinespecies.org/aphia.php?p=taxdetails&id=100698 on 2026-02-18.

53. M. H. Pettibone, "Polynoid Polychaetes Commensal With Antipatharian Corals," *Proceedings of the Biological Society of Washington* 104, no. 11 (1991): 714–726.

54. M. H. Pettibone, "Polynoids Commensals With Gorgonian and Stylasterid Corals, With a New Genus, New Combinations, and New Species (Polychaeta; Polynoidae; Polynoinae)," *Proceedings of the Biological Society of Washington* 104, no. 11 (1991): 688–713.

55. D. Martin and T. A. Britayev, "Symbiotic Polychaetes: Review of Known Species," *Oceanography and Marine Biology: An Annual Review* 36 (1998): 217–340.

56. K. J. Eckelbarger, L. Watling, and H. Fournier, "Reproductive Biology of the Deep-Sea Polychaete *Gorgoniapolynoe caeciliae* (Polynoidae), a Commensal Species Associated With Octocorals," *Journal of the Marine Biological Association of the United Kingdom* 85, no. 6 (2005): 1425–1433.

57. T. A. Britayev, J. Gil, Á. Altuna, M. Calvo, and D. Martín, "New Symbiotic Associations Involving Polynoids (Polychaeta, Polynoidae) From Atlantic Waters, With Redescriptions of *Parahololepidella Greeffi* (Augener, 1918) and *Gorgoniapolynoe caeciliae* (Fauvel, 1913)," *Memoirs of Museum Victoria* 71 (2014): 27–43.

58. S. Serpetti, M. L. Taylor, D. H. Green, A. D. Rogers, and G. L. J. Paterson, "Ecological Adaptations and Commensal Evolution of the Polynoidae (Polychaeta) in the Southwest Indian Ocean Ridge: A Phylogenetic Approach," *Deep Sea Research Part II: Topical Studies in Oceanography* 137 (2017): 273–281.

59. J. De Assis, J. Souza, M. Lima, G. Lima, R. Cordeiro, and C. Pérez, "Association Between Deep-Water Scale-Worms (Annelida: Polynoidae) and Black Corals (Cnidaria: Antipatharia) in the Southwestern Atlantic," *Zoologia* 36 (2019): 1–13.

60. T. Sugiyama, N. Jimi, and R. Goto, "Widening the Host Range of the Ectosymbiotic Scale-Worm *Asterophilia culcitae* (Annelida: Polynoidae) to Three Echinoderm Classes, With Data on Its Body Color Variation," *Plankton and Benthos Research* 15, no. 4 (2020): 289–295.

61. S. Taboada, A. S. Silva, L. Neal, et al., "Insights Into the Symbiotic Relationship Between Scale Worms and Carnivorous Sponges (Cladorhizidae, *Chondrocladia*)," *Deep Sea Research Part I: Oceanographic Research Papers* 156 (2020): 103191.

62. S. Taboada, A. Silva, S. Diez-Vives, et al., "Sleeping With the Enemy: Unravelling the Symbiotic Relationships Between the Scale Worm *Neopolynoe chondrocladiae* (Annelida: Polynoidae) and Its Carnivorous Sponge Hosts," *Zoological Journal of the Linnean Society* 193, no. 1 (2021): 295–318.

63. N. Jimi, N. Hookabe, T. Moritaki, T. Kimura, and S. Imura, "First Evidence of Male Dwarfism in Scale Worms: A New Species of Polynoidae (Annelida) From Hermit Crab and Molluscan Shells," *Journal of Zoological Systematics and Evolutionary Research* 59, no. 4 (2021): 801–818.

64. N. Jimi, N. Hookabe, S. P. Woo, and H. Kohtsuka, "Two New Genera and Species of Polynoidae (Annelida: Polychaeta) Associated With Sea Urchins," *Zoological Studies* 64 (2025): e21.

65. B. C. Gonzalez, V. M. Conde-Vela, and K. J. Osborn, "Synonymization of Two, Monotypic Black-Coral-Commensal Scale Worm Genera, Antipathipolyeunoa, Pettibone, 1991 and, Parahololepidella, Pettibone, 1969 (Polynoidae, Aphroditiformia). ZooKeys, 61-68," *ZooKeys* 1178 (2023), 61–68.

66. R. Periasamy, J. K. Palayil, and B. Ingole, "First Record of Sponge-Associated Deep-Sea Polychaete (Polynoidae: *Bathymoorea*) on the Ultraslow-Spreading Southwest Indian Ridge," *Deep Sea Research Part I: Oceanographic Research Papers* 191 (2023): 103923.

67. G. Fassio, "*Coriocella* and the Worms: First Record of Scale-Worm *Asterophilia* cf. *culcitae*, Ectosymbiotic on a Mollusc," *Diversity-Basel* 16, no. 1 (2024): 65.

68. G. C. Bourne, "The Anthozoa," in *A Treatise on Zoology. Part II. The Porifera and Coelenterata*, ed. E. R. Lankester, (Adam & Charles Black, 1900): 1–84.

69. J. V. F. Lamouroux, "Extrait d'un mémoire sur la classification des Polypiers coralligènes non entièrement pierreux," *Nouveau Bulletin scientifique de la Société Philosophique* 3 (1812): 181–188.

70. R. Owen, "Lectures on the Comparative Anatomy and Physiology of the Invertebrate Animals," (1843).

71. T. Molodtsova, T. A. Britayev, and D. Martin, "Cnidarians and Their Polychaete Symbionts," in *The Cnidaria, Past, Present and Future: The World of Medusa and her Sisters*, eds. S. Goffredo and Z. Dubinsky, (Springer International Publishing, 2016): 387–413.

72. R. Hertwig, *Die Actinien der Challenger Expedition* (Gustav Fischer, 1882).

73. T. A. Britayev, "Life Cycle of the Symbiotic Scaleworm *Arctonoe vittata* (Polychaeta: Polynoidae)," *Ophelia Supplement* 5 (1991): 305–312.

74. G. Johnston, "Illustrations in British Zoology," *Magazine of Natural History and Journal of Zoology, Botany, Mineralogy, Geology, and Meteorology* 5 (1832): 163-164.

75. A. E. Grube, "Beschreibungen Neuer Oder Wenig Bekannter Anneliden," *Archiv für Naturgeschichte* 21, no. 1 (1855): 81–136.

76. C. Linnaeus, *Fauna Suecica Sistens Animalia Sueciae Regni: Distributa per Classes, Ordines, Genera, Species, Cum Differentiis Specierum, Synonymis Auctorum, Nominibus Incolarum, Locis Natalium, Descriptionibus Insectorum* (Stockholmiae, (Editio Altera, Auctior), 1761).

77. C. S. Rafinesque, *Analyse de la Nature ou Tableau de l'univers et des Corps Organisés* (Palermo, 1815).

78. J. Li, L. Zhang, M. Wang, and X. Wu, "A New Species of, *Macellicephaloides*, Uschakov, 1955 (Annelida, Polynoidae) From Cold Seeps in the South China Sea: Insights Into the Taxonomy and Phylogeny of Macellicephaloides and Related Genera," *Current Issues in Molecular Biology* 47, no. 11 (2025): 897.

79. A. Murray, I. Burghardt, L. M. Gunton, N. M. Nizar, M. C. Nikolic, and R. S. Wilson, "Polynoidae (Annelida) From Bathyal and Abyssal Depths in Southern and Eastern Australia," *Records of the Australian Museum* 77, no. 4 (2025): 193–269.

80. X. Wu, Q. Kou, Y. Sun, W. Zhen, and K. Xu, "Morphology, Phylogeny and Evolution of the Rarely Known Genus, *Admetella*, McIntosh, 1885 (Annelida, Polynoidae) With Recognition of Four New Species From Western Pacific Seamounts," *Journal of Zoological Systematics and Evolutionary Research* 2024, no. 1 (2024).

81. J. R. Hanley and M. Burke, "Polychaeta Polynoidae: Scaleworms of the Chesterfield Islands and Fairway Reefs, Coral Sea," *Mémoires du Muséum National d'Histoire Naturelle* 151 (1991): 9–82, Série A.

82. X. Wu, W. Zhen, Q. Kou, and K. Xu, "Revaluation of the Systematic Status of *Branchinotogluma* (Annelida, Polynoidae), With the Establishment of Two New Species," *Journal of Zoological Systematics and Evolutionary Research* 1490800 (2023).

83. B. C. Gonzalez, A. Martínez, K. Worsaae, and K. J. Osborn, "Morphological Convergence and Adaptation in Cave and Pelagic Scale Worms (Polynoidae, Annelida)," *Scientific Reports* 11, no. 1 (2021): 10718.

## Supporting Information

Additional supporting information can be found online in the Supporting Information section. (*Supporting Information*)

Table S1. Best partitioning schemes and models of the 17-gene matrix selected by ModelFinder. Table S2. Morphological dataset of the studied polynoids used for ancestral state reconstruction analyses. Lateral antennae: State 0, absent; State 1, present. Lateral antennae terminally or subterminally inserted: State 0, absent; State 1, present. Lateral antennae ventrally or terminoventrally inserted: State 0, absent; State 1, present. Deeply incised neuropodia: State 0, absent; State 1, present. Table S3. Percentage estimates of Kimura's 2-parameter pair-wise genetic distances of 16S rRNA (528 bp, below diagonal) and COI (1540 bp, above diagonal) gene sequences among three species of *Alentiana* Hartman, 1942. Figure S1. Sampling localities of *Alentiana* in the tropical western Pacific. M4, M5, and M8 are adjacent seamounts in the Caroline Seamount Chain; Seamount Kocebu is positioned ~1700 km northeast of the aforementioned three seamounts. Figure S2. Bayesian inference (BI) tree of *Alentiana* and related taxa inferred from the concatenated 17-gene matrix partitioned by gene and codon. Figure S3. Maximum likelihood (ML) tree of *Alentiana* and related taxa inferred from the concatenated 17-gene matrix partitioned by gene and codon. Figure S4. Dorsal view of the left side of segments 32–39 of *Alentiana barnichae* sp. nov. (paratype, MBM287245), showing that the terminal elytra only extend to segment 37.